青藏高原东南部地区岩石圈结构与形变

Lithospheric structure and deformation of southeastern Tibetan Plateau

姚 华 建

中国科学技术大学 地球和空间科学学院

合作者：Rob van der Hilst (MIT)，Hui Huang (MIT)

M. de Hoop (Purdue Univ), Jean-Paul Montagner (IPGP)

刘启元，李昱（中国地震局地质研究所）

2014年5月23日 台湾国立中央大学

Where is USTC, Hefei, Anhui province ......

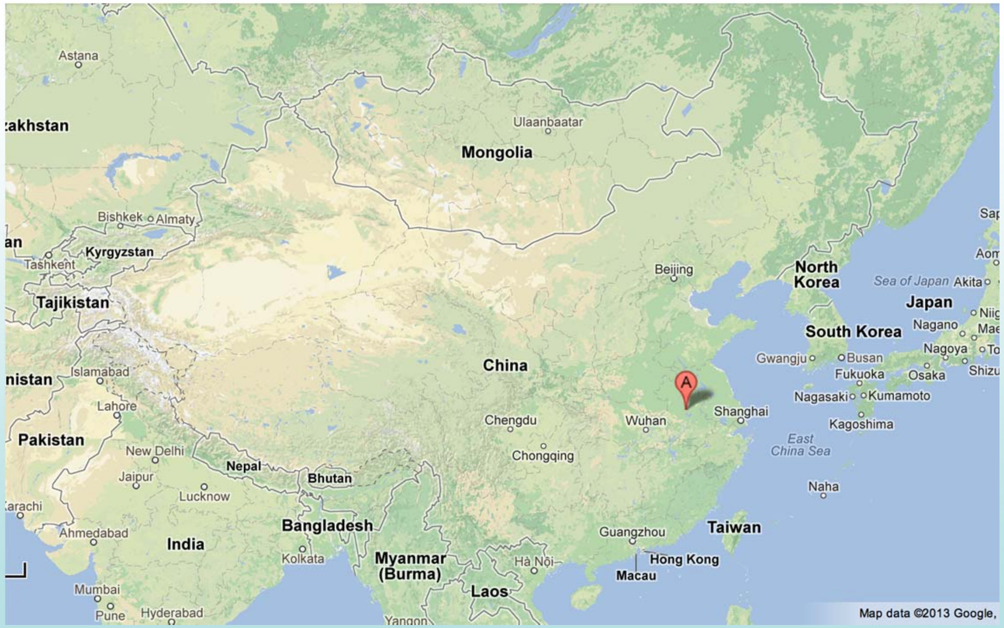

Tectonic evolution of Tibetan Plateau

continental collision between the Indian and Eurasian plates

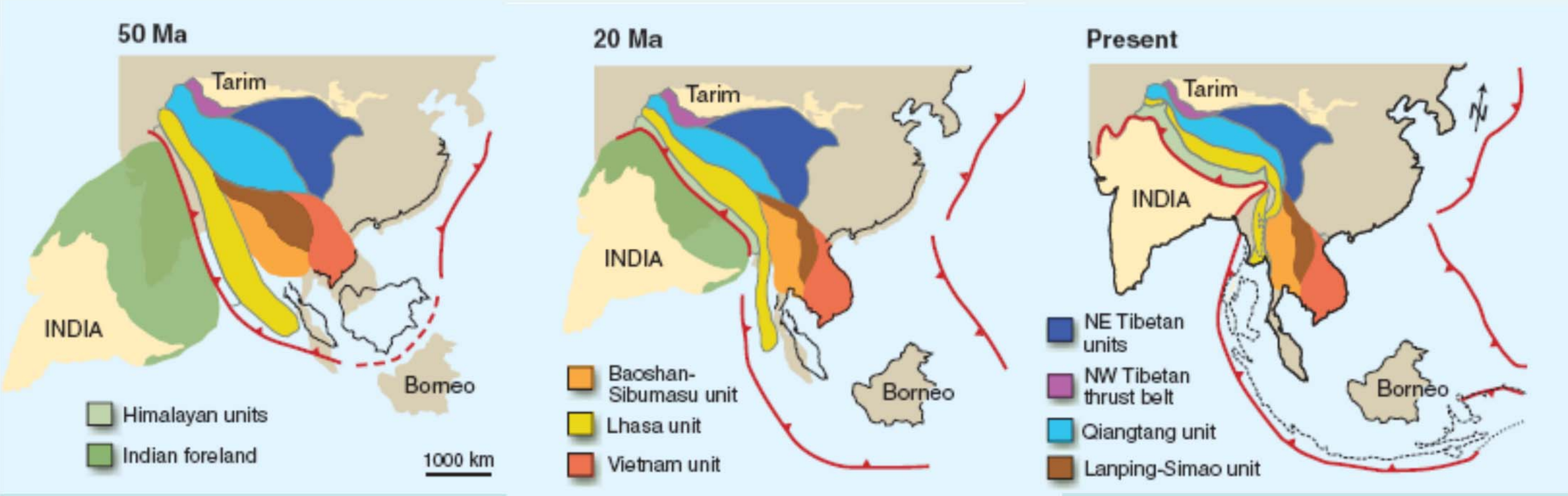

Royden et al., 2008, Science

Consequences of India-Eurasia collision

- Surface elevation ~ 5 km, crustal thickness 70~80 km
- Eastward extrusion of material from central Tibet
- Active faults and numerous continental earthquakes
- Highly deformed Tibetan Plateau crust

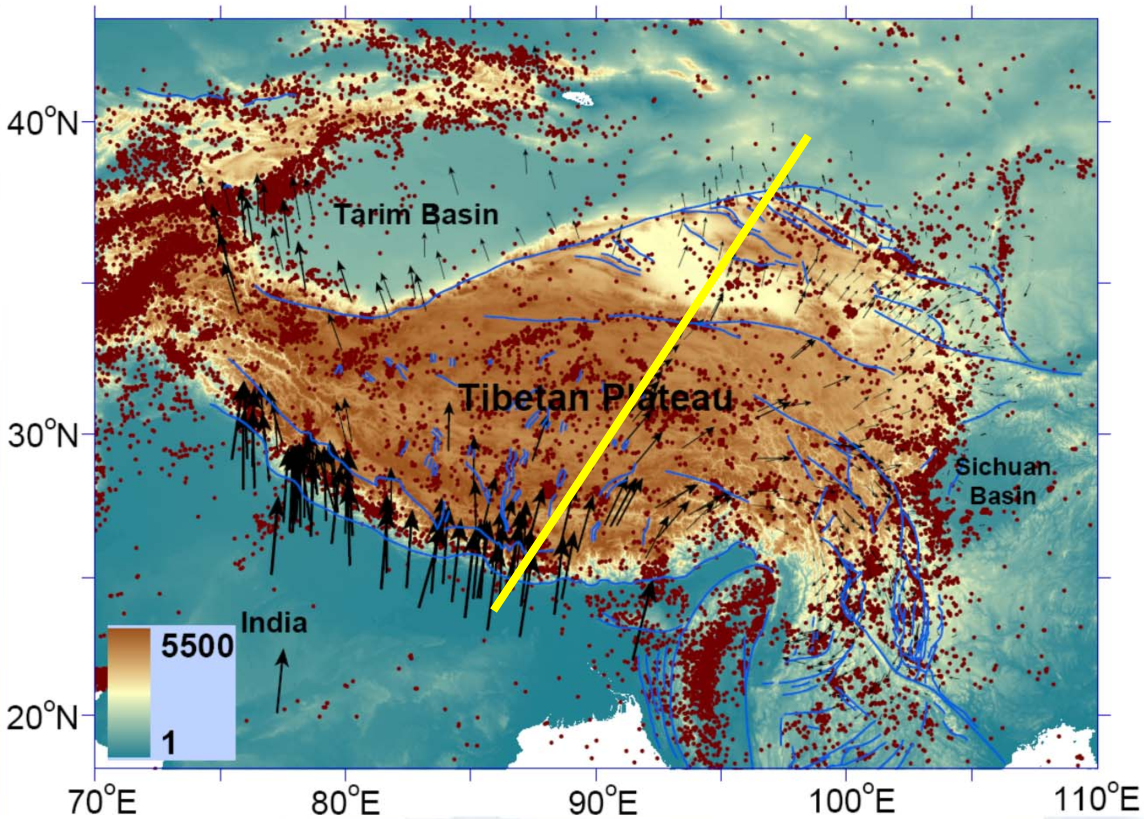

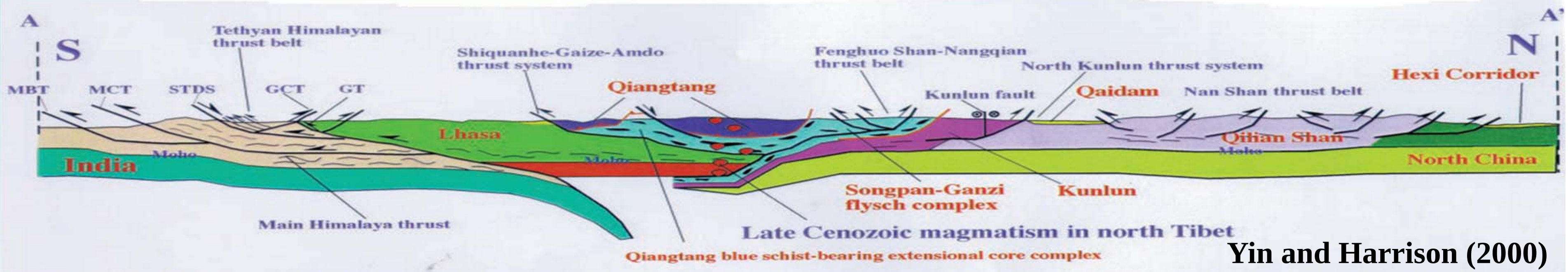

Yin and Harrison (2000)

- **Debates on deformation mechanisms of the Tibetan Plateau**

two end member models:

rigid block extrusion (Tapponnier et al., 1982),

lower crust channel flow (Royden et al., 1997)

Coupled crust-mantle

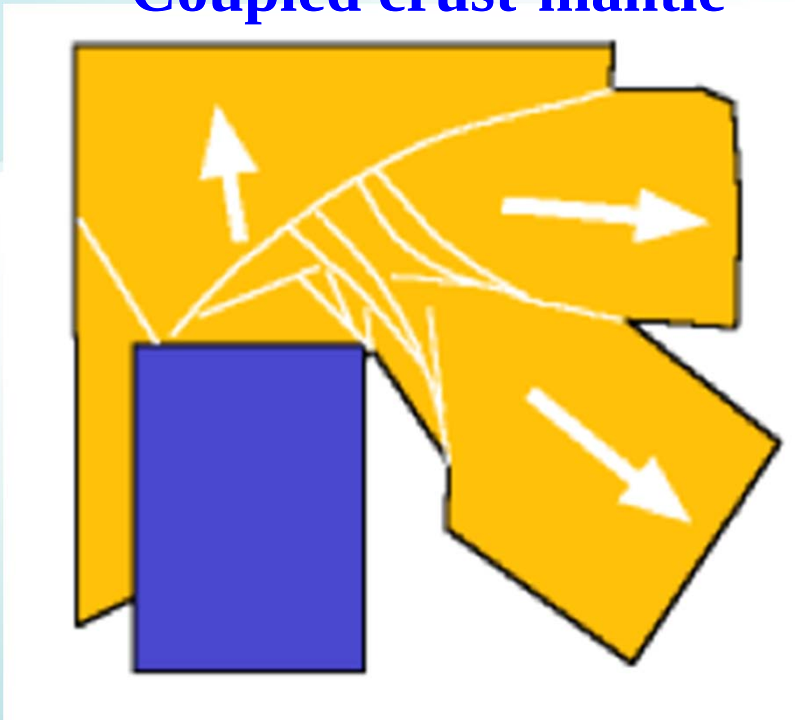

Decoupled crust-mantle

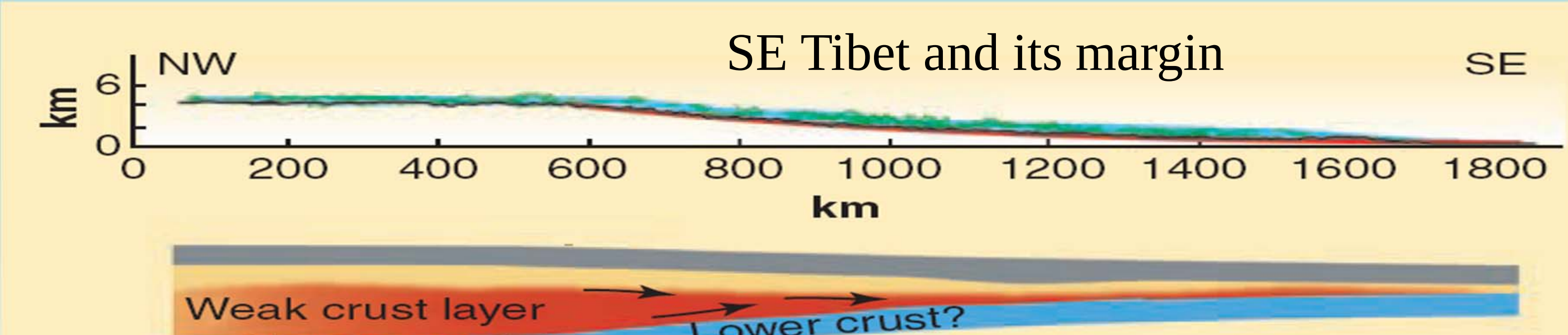

Royden, Burchfiel, van der Hilst, 2008, Science

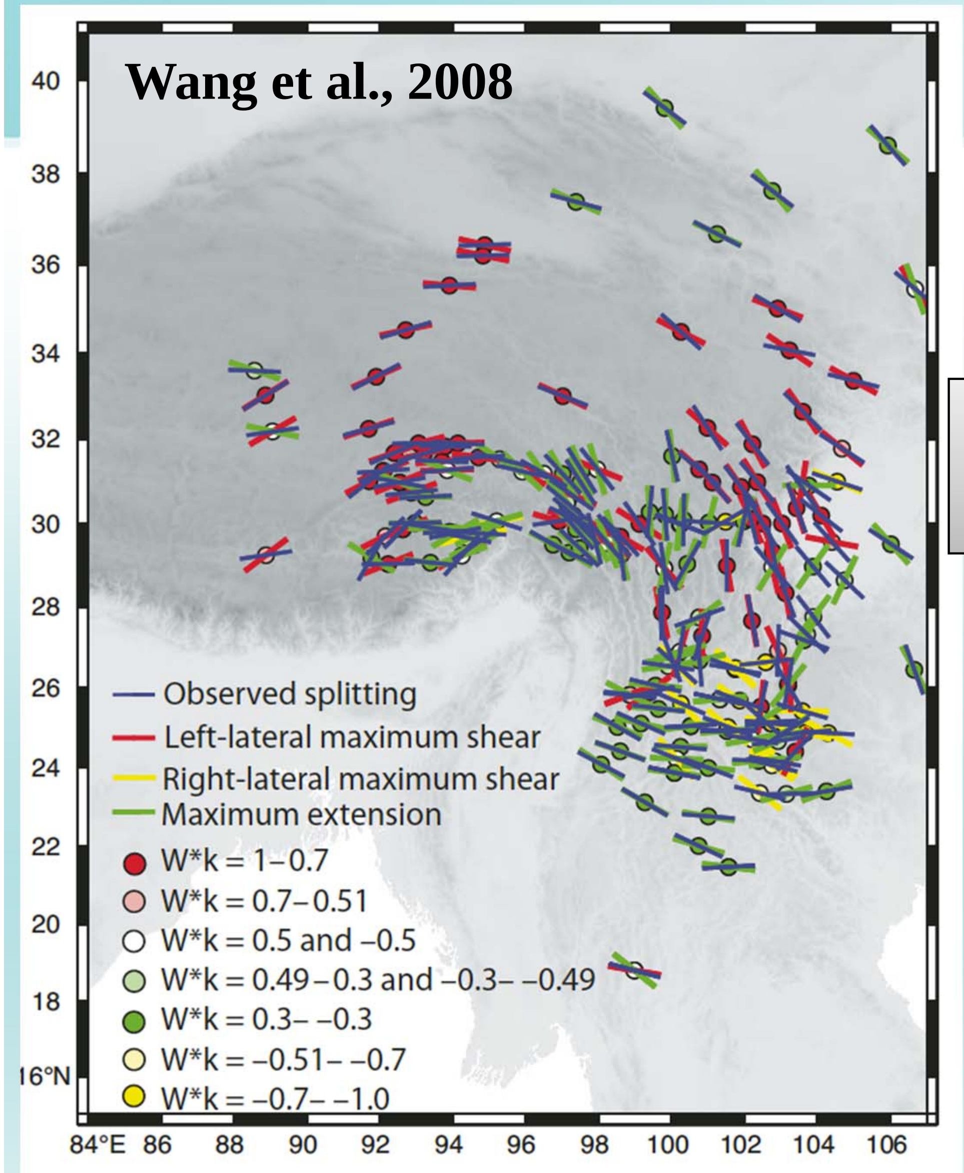

Crust-mantle deformation

GPS V field

SKS splitting

Surface strain rate field

?

?

Crust deformation

Upper mantle deformation

Vertically coherent deformation

(Flesch et al., 2005; Sol et al., 2007, Wang et al., 2008)

Teleseismic shear wave splitting in SE Tibet：～1 s

Crust shear wave splitting from receiver function：～0.5－0.9 s

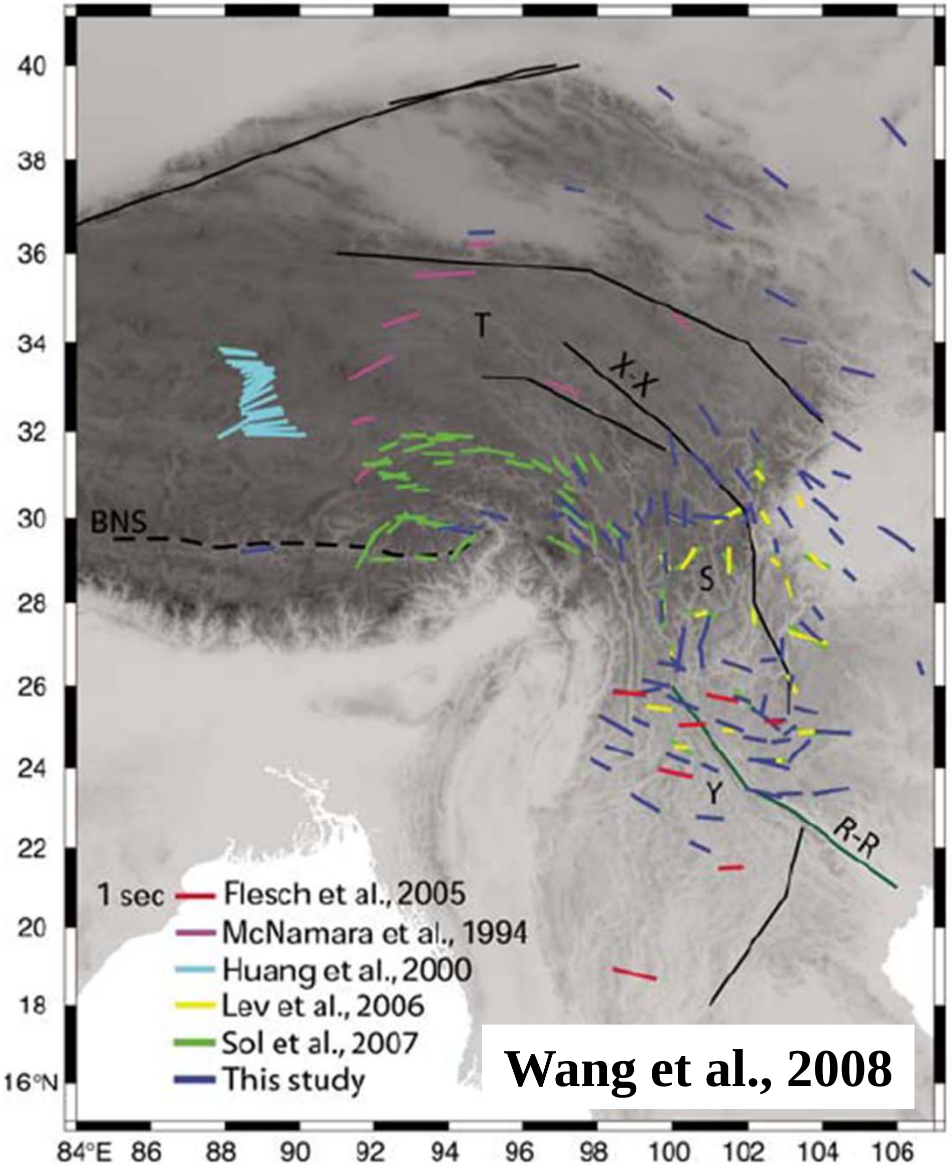

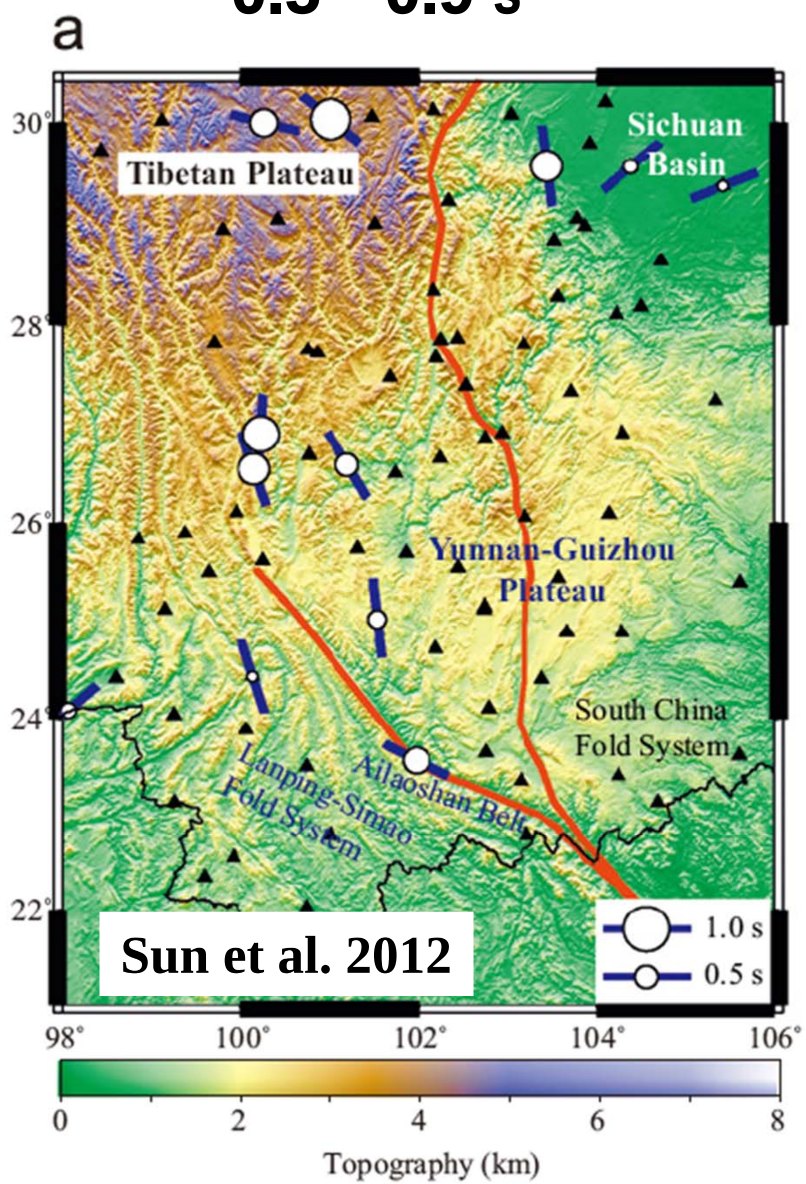

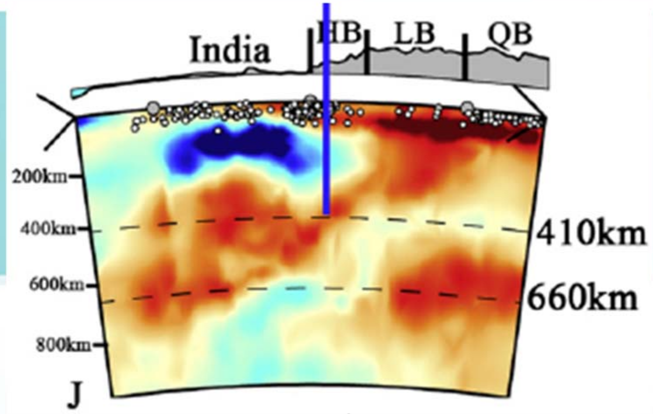

Southeastern Tibetan Plateau

complicated tectonic processes and deformation history

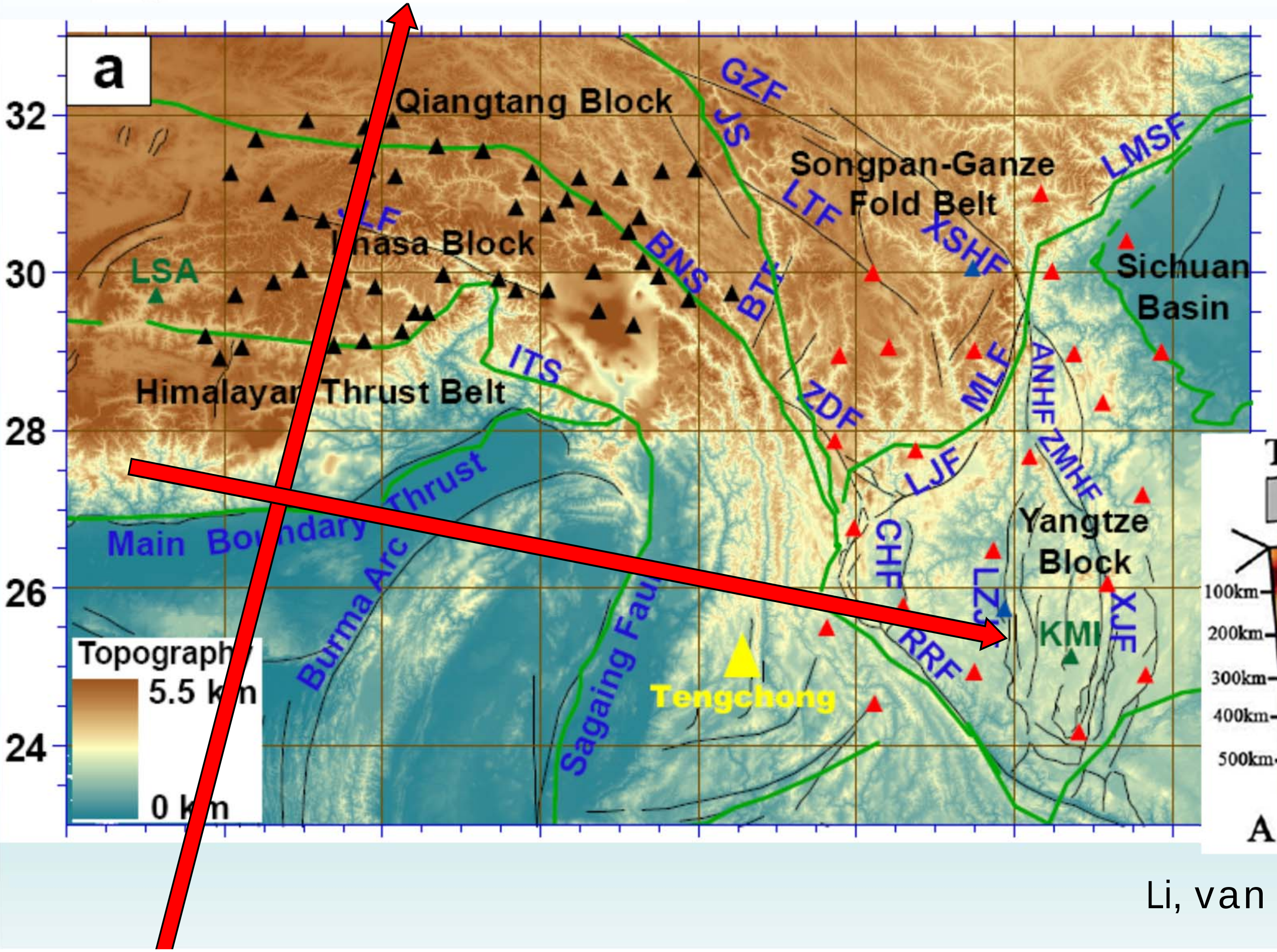

Indian subduction,

Burma subduction,

Obstruction of rigid Sichuan Basin

Strike-slip faults, suture

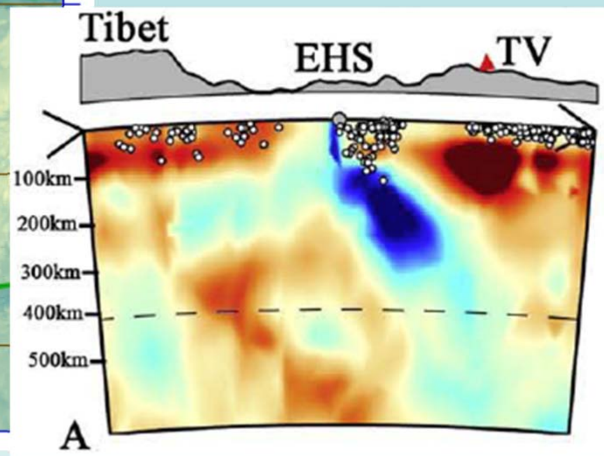

Li, van der Hilst et al., 2008

75 stations
Ambient Noise＋Earthquake
surface wave tomography

3-D crust & upper mantle
Vs + anisotropy

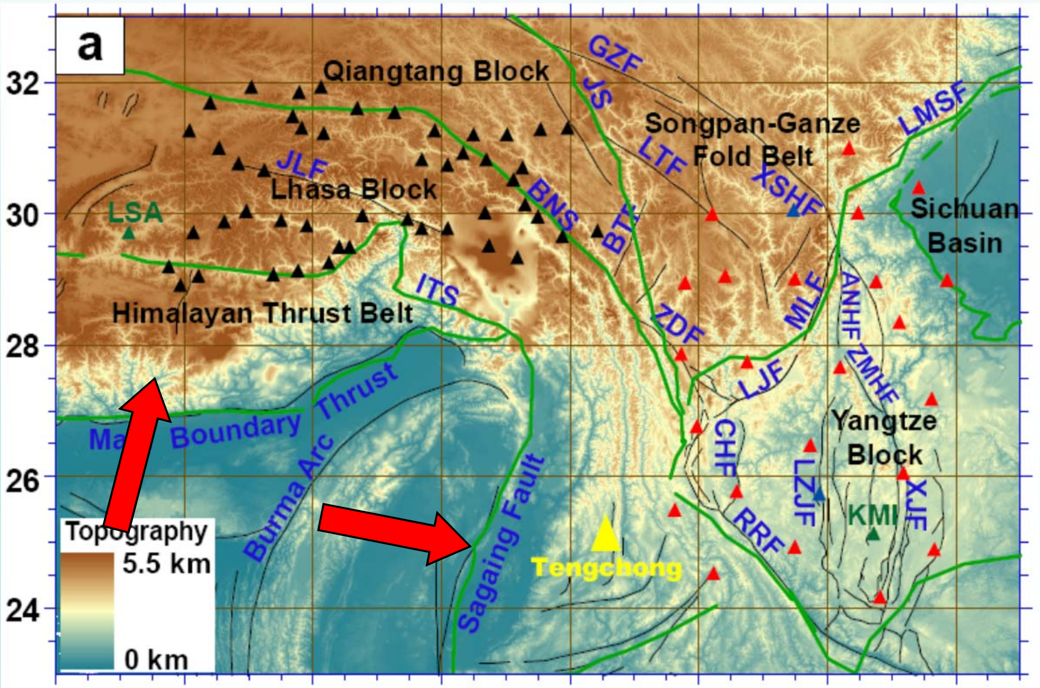

Yao, et al., 2008, Geophy. J. Int.
Yao, et al., 2010, J. Geophys. Res.
Huang, 2010, Geophys. Res. Lett.
Yao 2012, Earthquake Sci，Liu et al, 2004 Nature Geoscience

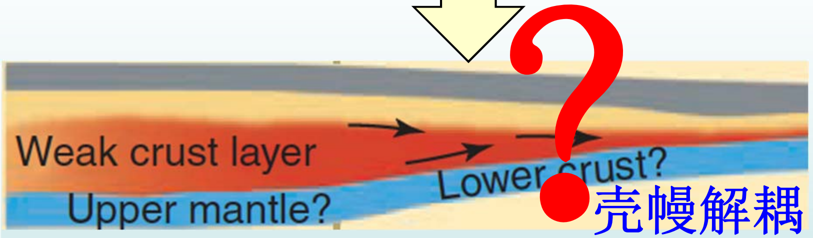

Lower crust flow
(Royden et al, 1997)

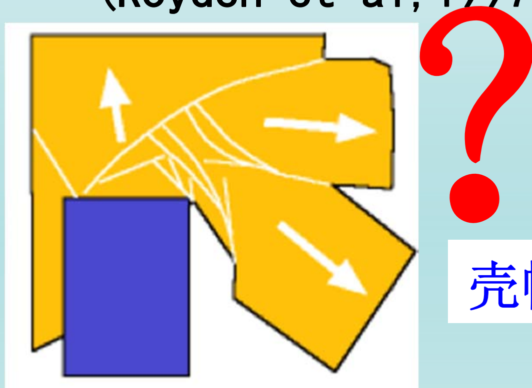

壳幔耦合

Rigid block extrusion
(Tapponnier et al, 1982)

1. Data and Surface-wave Dispersion Analysis
(Ambient Noise + Earthquake Data)

Ambient Noise Tomography

Ambient Noise Cross-Correlation → 2004 → Green's function between receivers → 2005 → Velocity structure beneath the receiver array

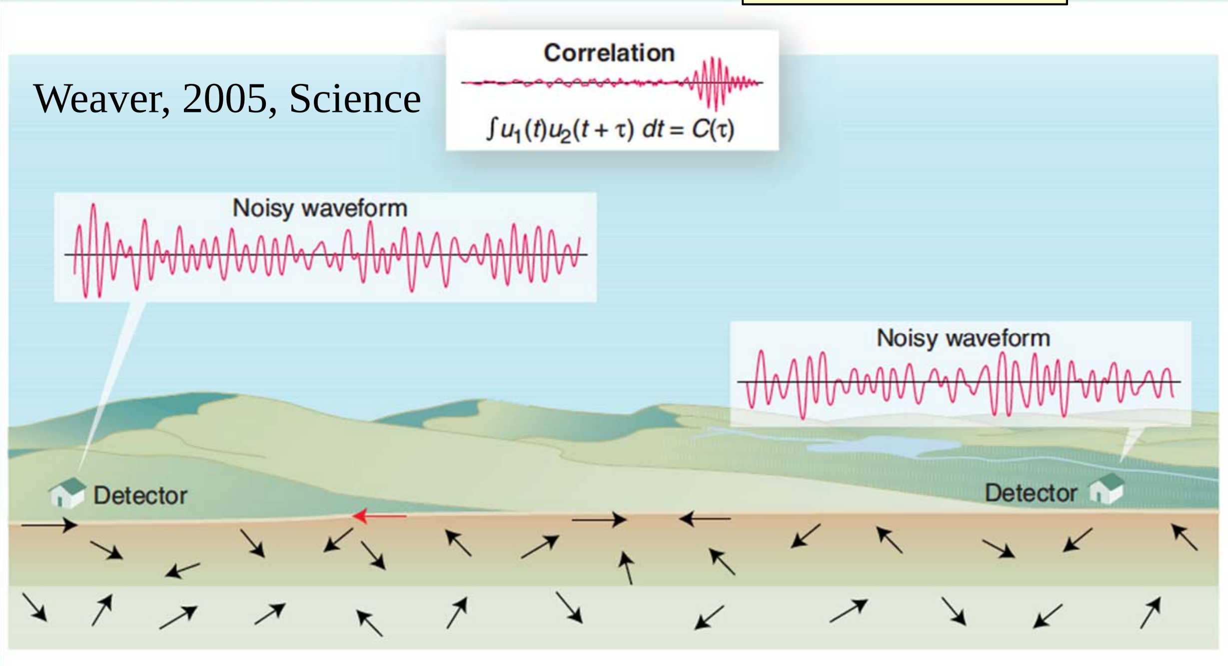

Advantages

1、no need of earthquakes or explosives

2、high-resolution crustal/shallow surface images beneath the array

One of the Biggest Breakthroughs in Structural Seismology in 21st Century

Ambient noise cross-correlation for the recovery of surface wave Green's function (Campillo & Paul, 2003; Shapiro & Campillo, 2004)

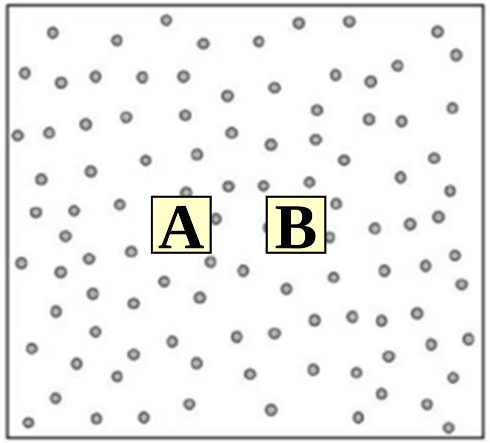

(noise) cross-correlation function

$$\frac{dC_{AB}(t)}{dt} = -\hat{G}_{AB}(t) + \hat{G}_{BA}(-t) \approx -G_{AB}(t) + G_{BA}(-t)$$

Empirical Green's function (EGF) from a 'source' at A and a receiver at B

Real Green's function from a 'source' at A and a receiver at B

Cases of uneven distribution of noise sources

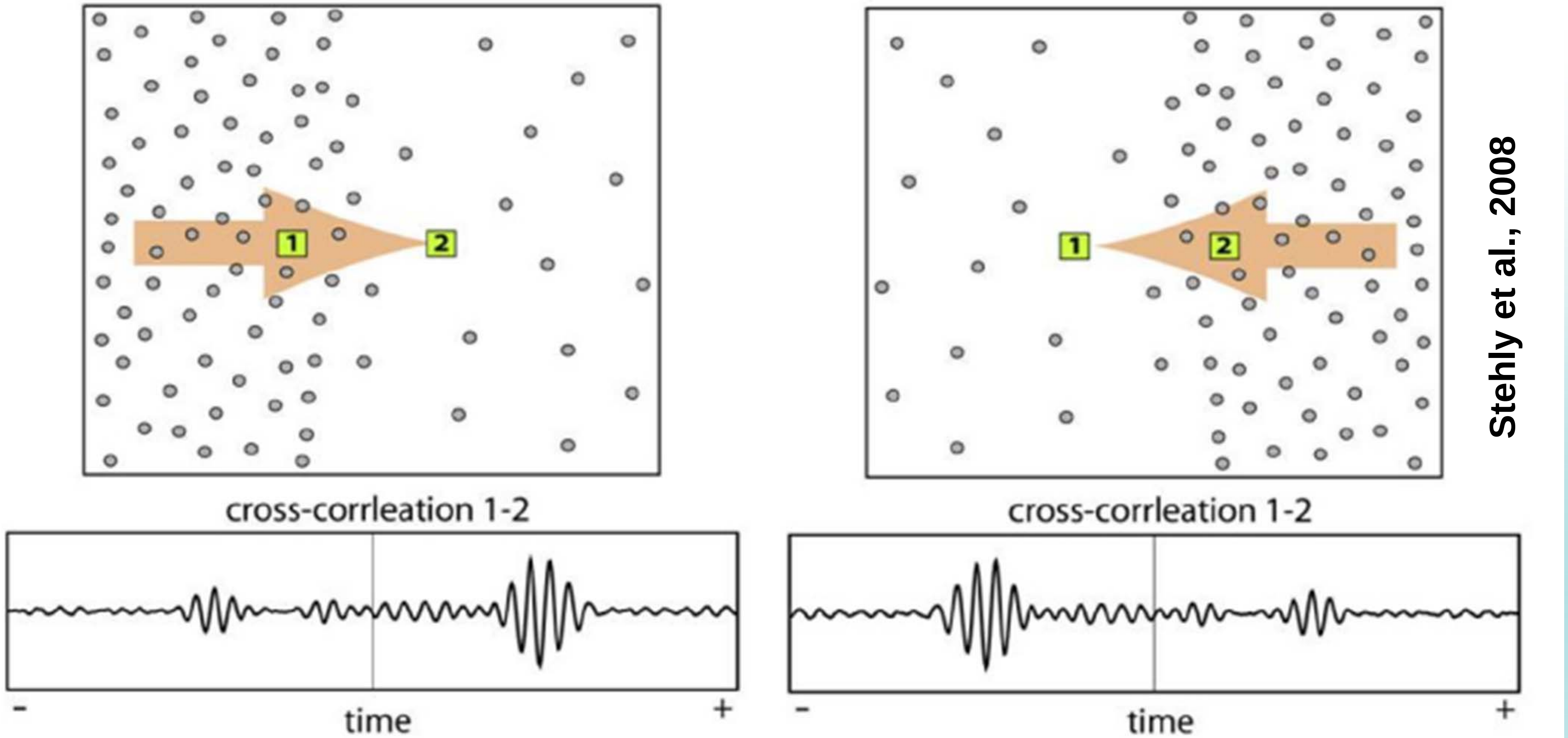

Stehly et al., 2008

Smooth distribution of ambient noise energy will result in relatively small bias of travel times (usually < 1%, Yao & van der Hilst, 2009) although the amplitudes of CFs may vary a lot.

Ambient Noise Cross-Correlation

Z-Z → Rayleigh **T-T → Love**

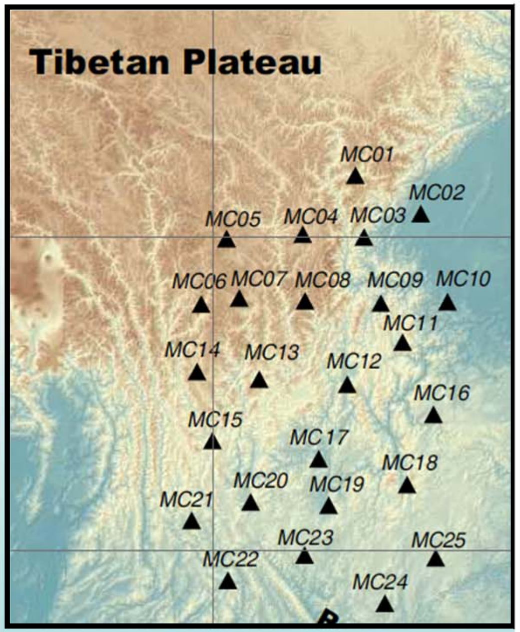

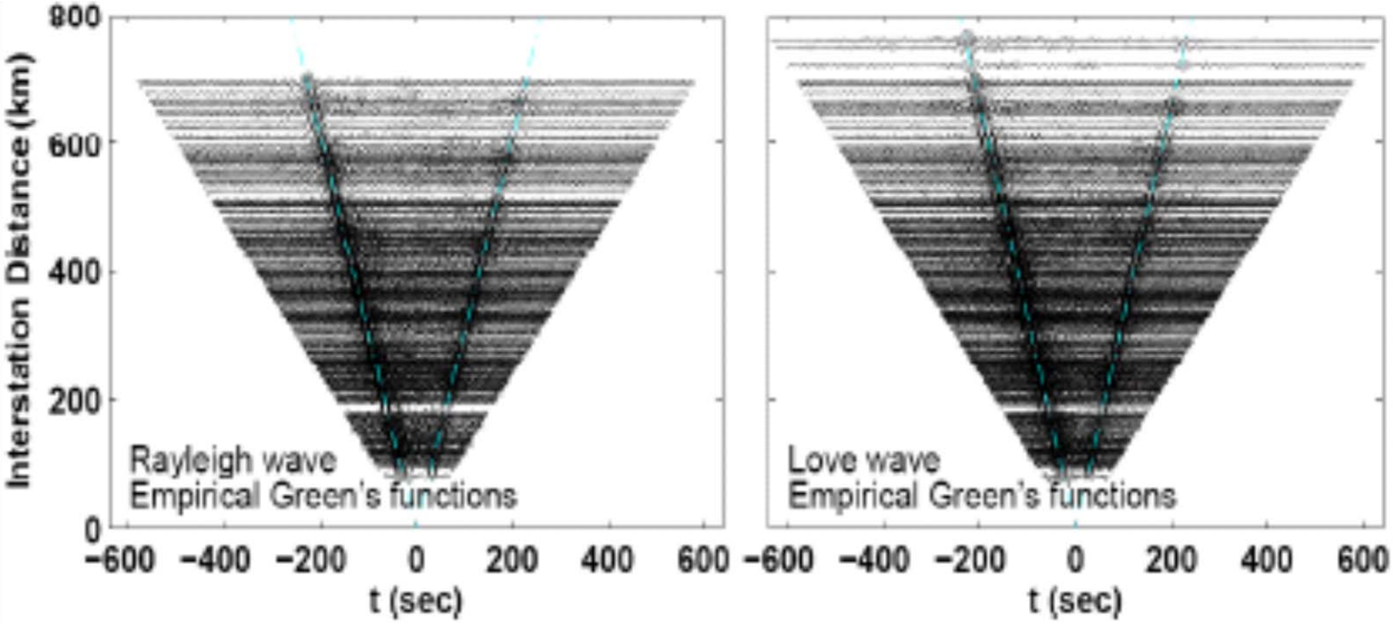

Inter-station ambient noise cross-correlation (10 – 40 s)
→Surface wave propagation between stations
→ Vsv / Vsh crustal structure beneath the array

Phase Velocity Dispersion Measurements

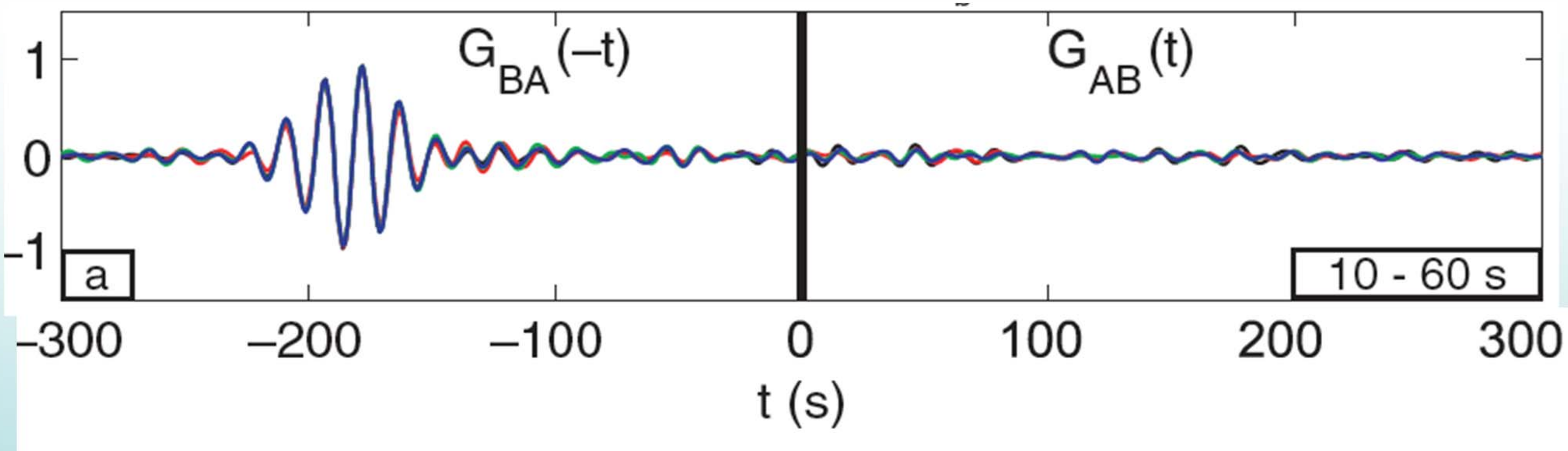

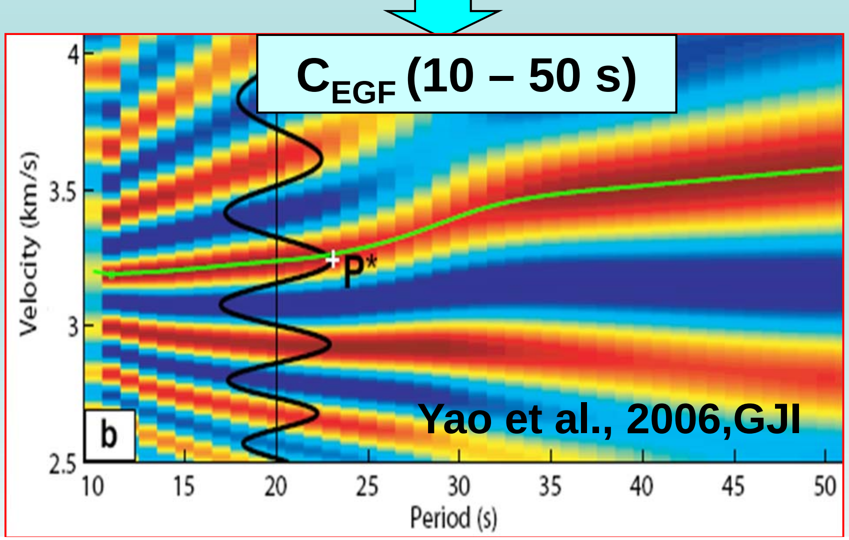

Advantages of phase velocity measurements over group velocity measurements

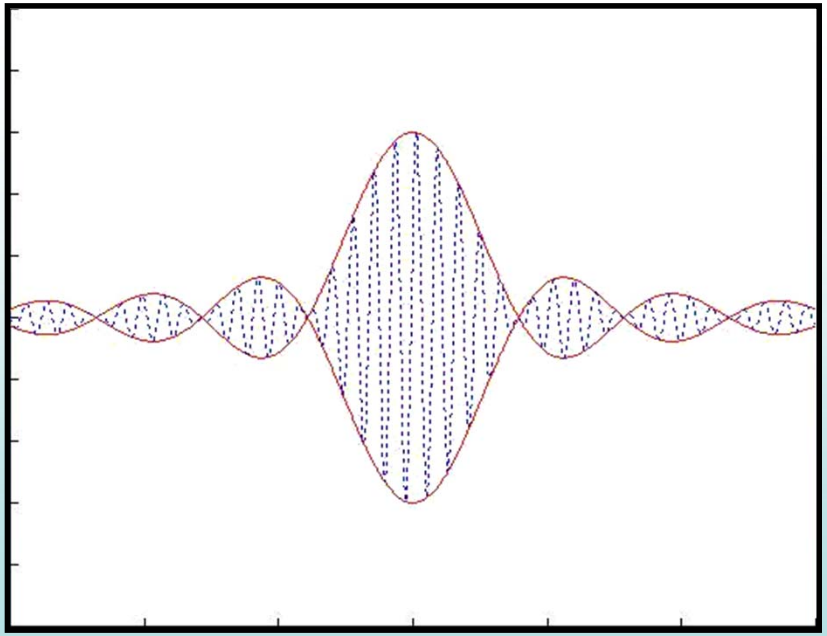

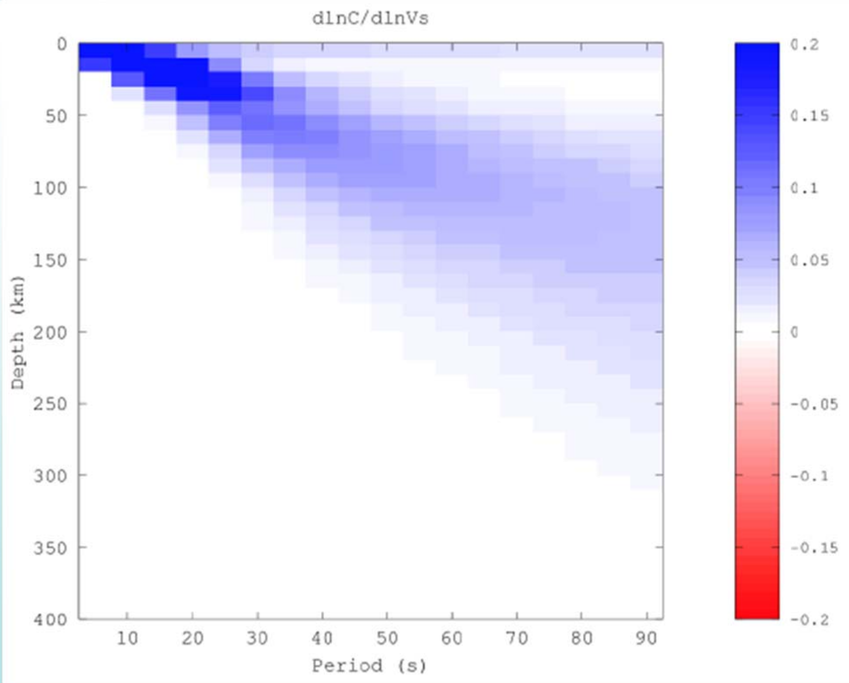

1. Better accuracy at longer periods

(e.g., T=30s ： error in group v ～ 2 x error in phase v)

2. Easy to combine with inter-station phase velocity measurements from earthquake data

ambient noise：5－40 s （5－70 km）

EQ surface wave：20－150 s （20－250 km）

Monthly Rayleigh wave phase velocity maps from vertical component EGFs

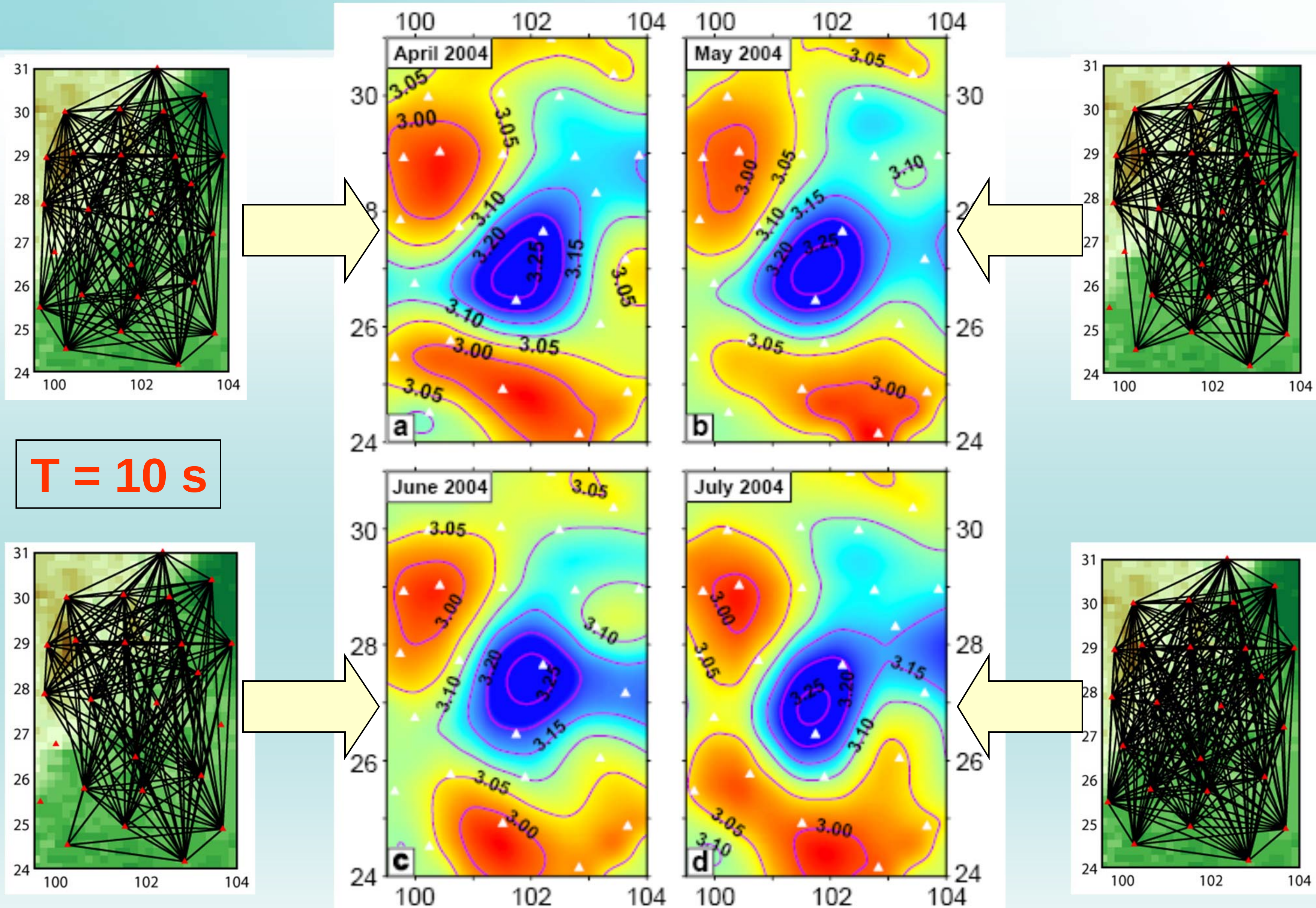

T = 10 s

Yao, van der Hilst, de Hoop, 2006

Earthquake Data: Two-station analysis

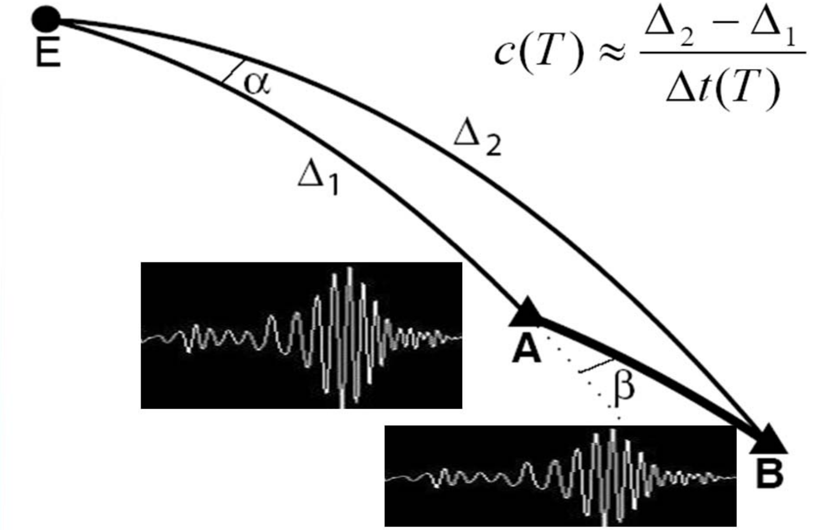

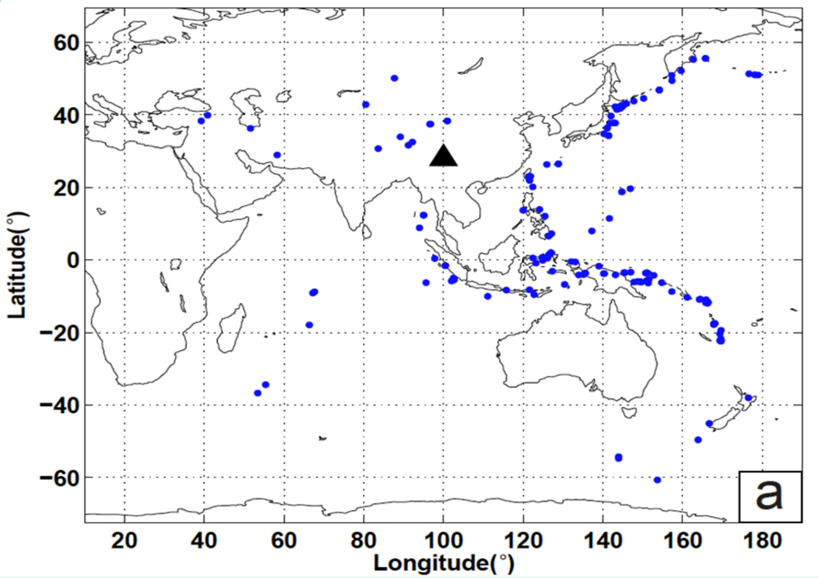

Teleseismic surface waves

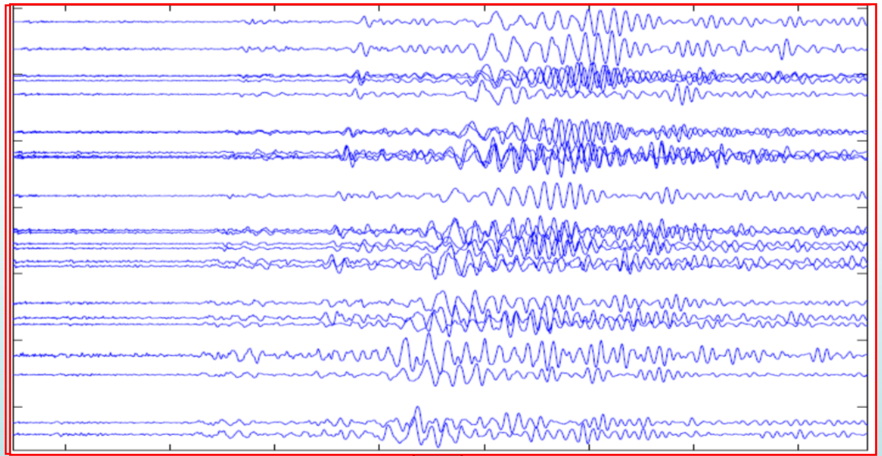

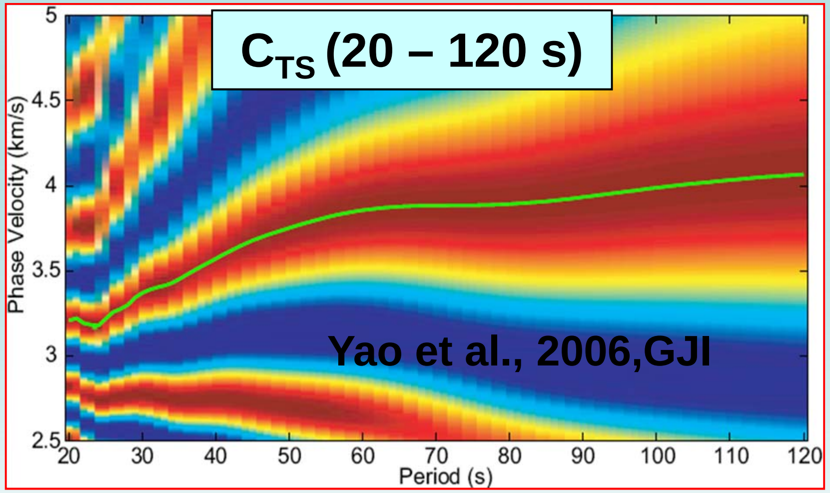

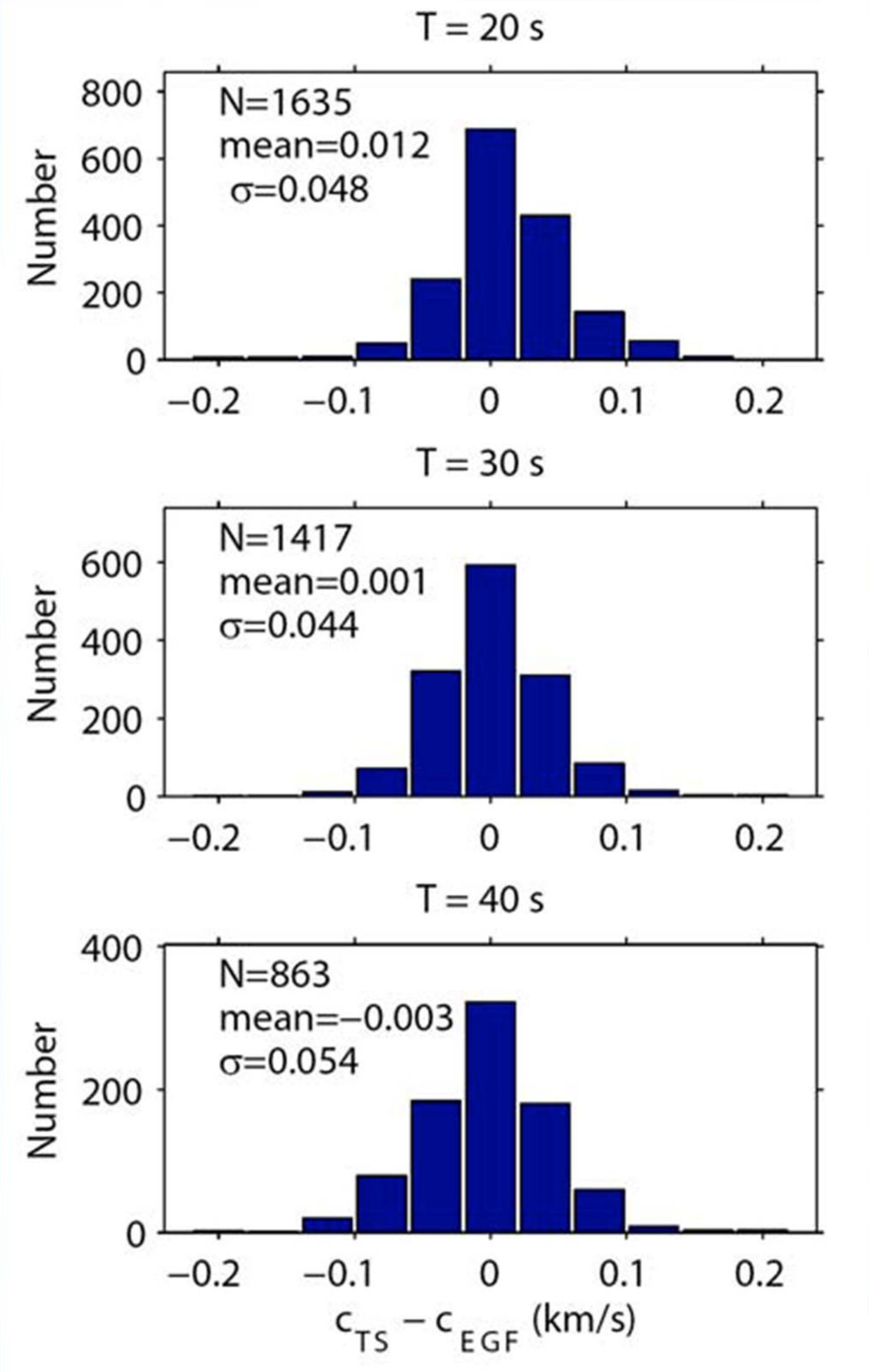

Phase velocity comparison between EGF and TS methods

Similar in the overlapping periods (20-40 s)

For T > 40 s, their differences become much larger

Yao et al (2010)

2. Inversion for Lithospheric Structure and Anisotropy

Ambient Noise Cross-correlation

phase velocity dispersion from EGF at shorter periods (10 – 40 s)

Teleseismic Surface-wave Two-station Analysis

phase velocity dispersion from TS at longer periods (20 – 150 s)

EGF + TS average interstation dispersion (10 – 150 s)

2-D phase velocity maps (T = 10 – 150 s)

Crustal and upper mantle Vs structure

Inversion for shear velocity structure, azimuthal, and radial anisotropy

- Step 1: inter-station phase v → azimuthally anisotropic phase velocity maps

$$c(\omega,\psi)=c_0(\omega)[1+a_0(\omega)+a_1(\omega)\cos 2\psi+a_2(\omega)\sin 2\psi]$$

- Step 2: Rayleigh phase velocity maps → 3-D **Vsv** structure

  Love phase velocity maps → 3-D **Vsh** structure

  (using Neighborhood algorithm)

- Step 3: Shear velocity radial anisotropy: 2*(Vsh – Vsv)/(Vsh + Vsv)

- Step 4: Shear velocity azimuthal anisotropy:

$$\delta c_R(x,y,\omega,\psi)\approx\int_0^H\left[\frac{\partial c_R}{\partial L}\left(\delta L+G_c\cos 2\psi+G_s\sin 2\psi\right)\right]\frac{dz}{\Delta h}$$

Step 2

Transverse isotropic V_{sv}: $\beta_{SV}=\sqrt{L/\rho}$

Mag. of V_{sv} azimuthal aniso : $A_{SV}=\frac{1}{2L}\sqrt{(G_c)^2+(G_s)^2}$

Fast axis of V_{sv} azimuthal aniso : $\phi=\frac{1}{2}\tan^{-1}(G_s/G_c)$

Example of inversion for azimuthally anisotropic phase velocity maps

~2300 paths

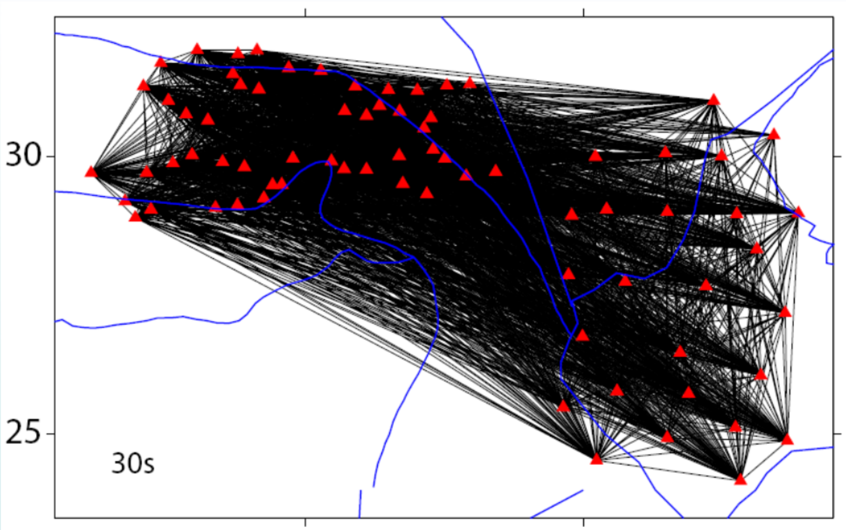

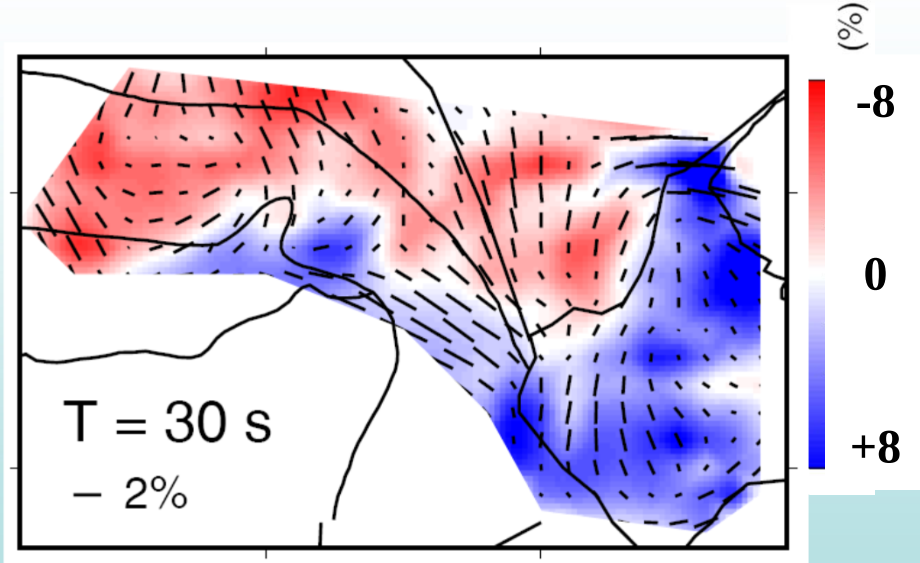

Yao, van der Hilst, Montagner, 2010,JGR

Checkerboard resolution tests

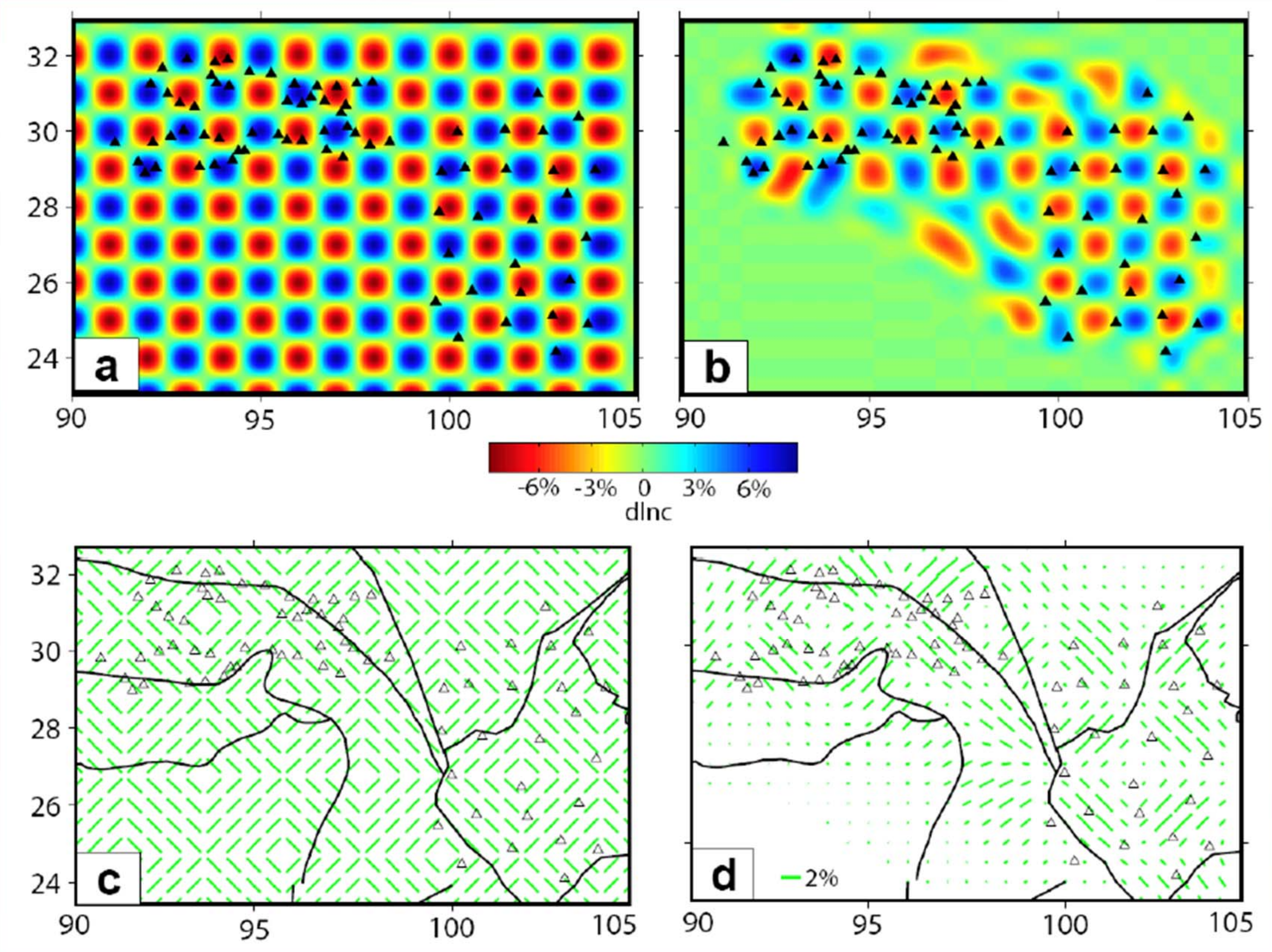

Yao, van der Hilst, Montagner, 2010,JGR

Examples of inversion results **(Radial Anisotropy)**

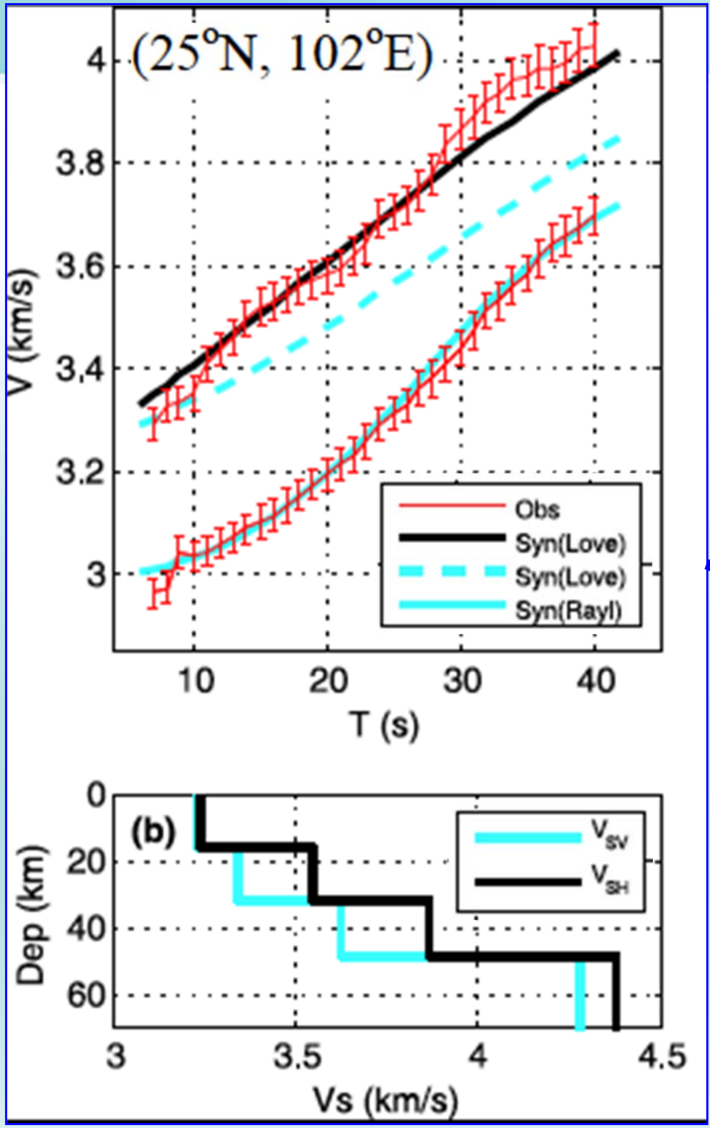

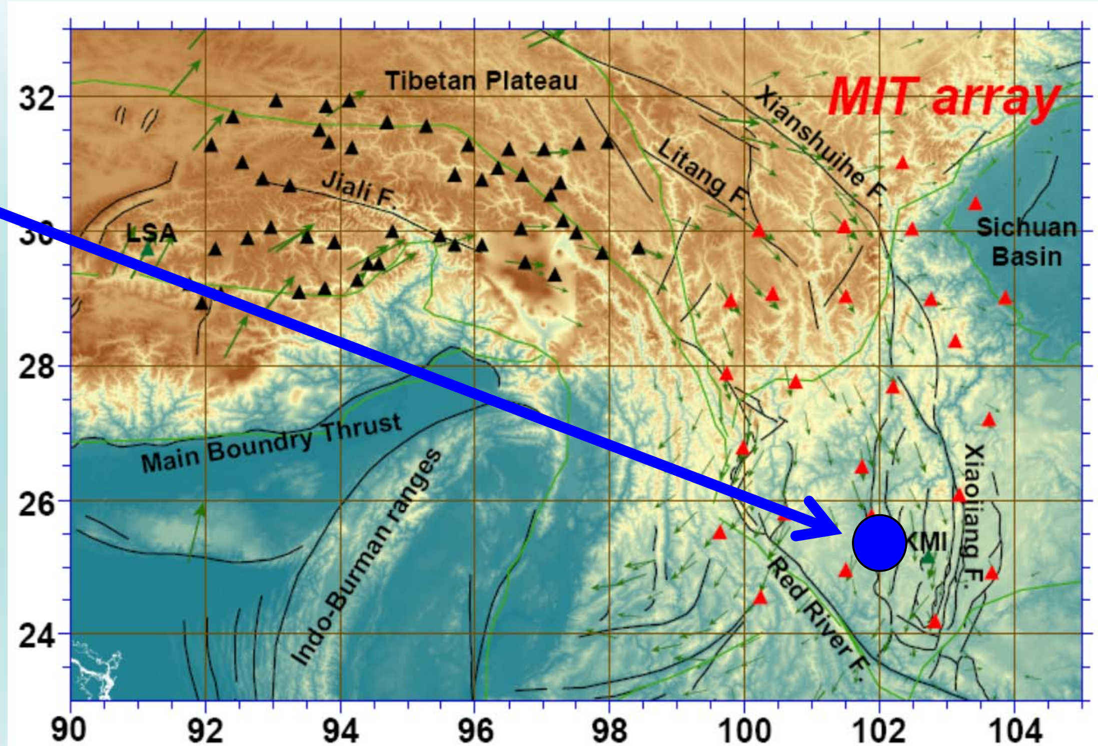

Examples of inversion results **(Azimuthal Anisotropy)**

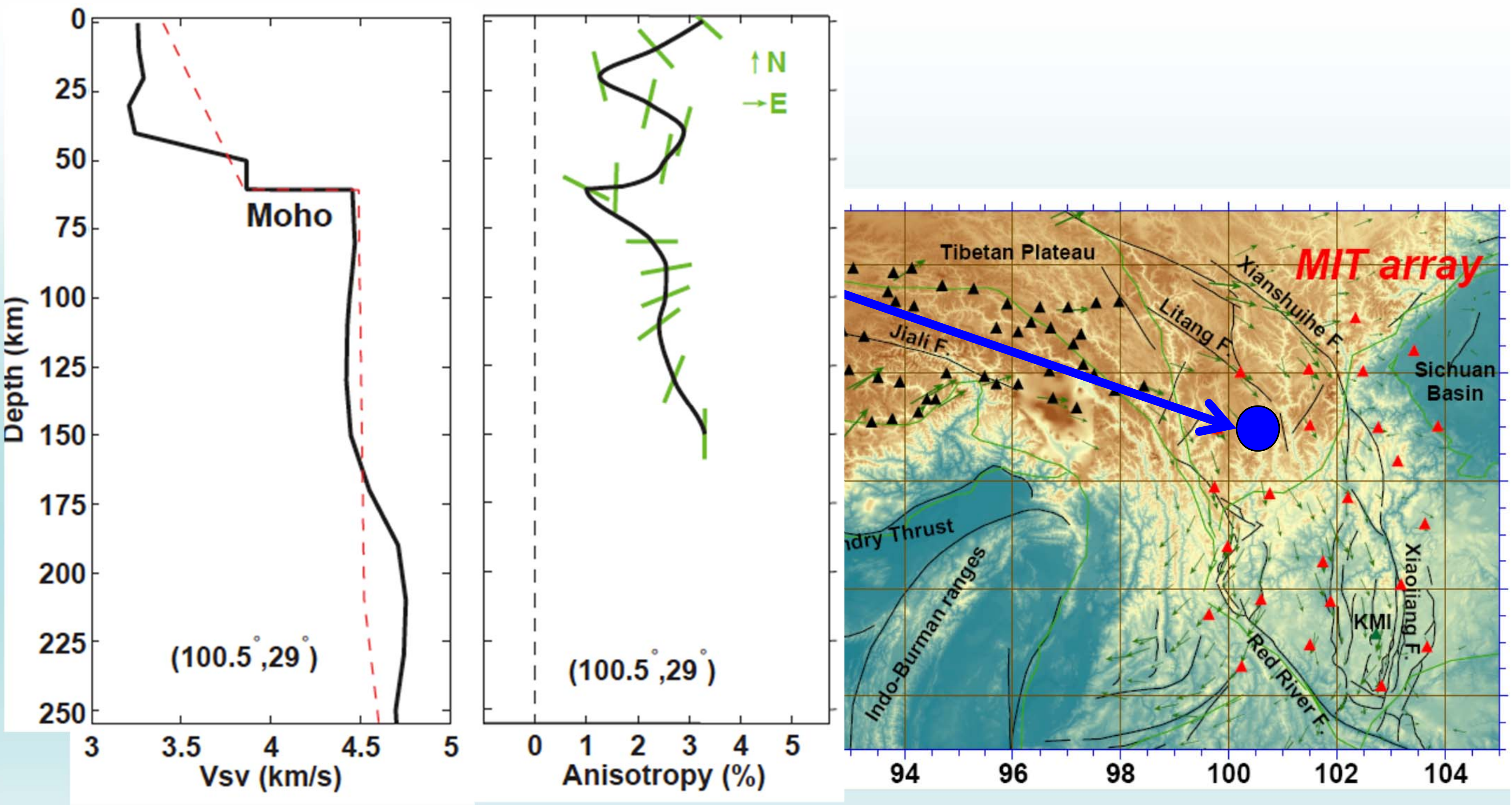

3. Results and Discussions

(1) Middle/Low Crustal Low Velocity Zones (LVZs)

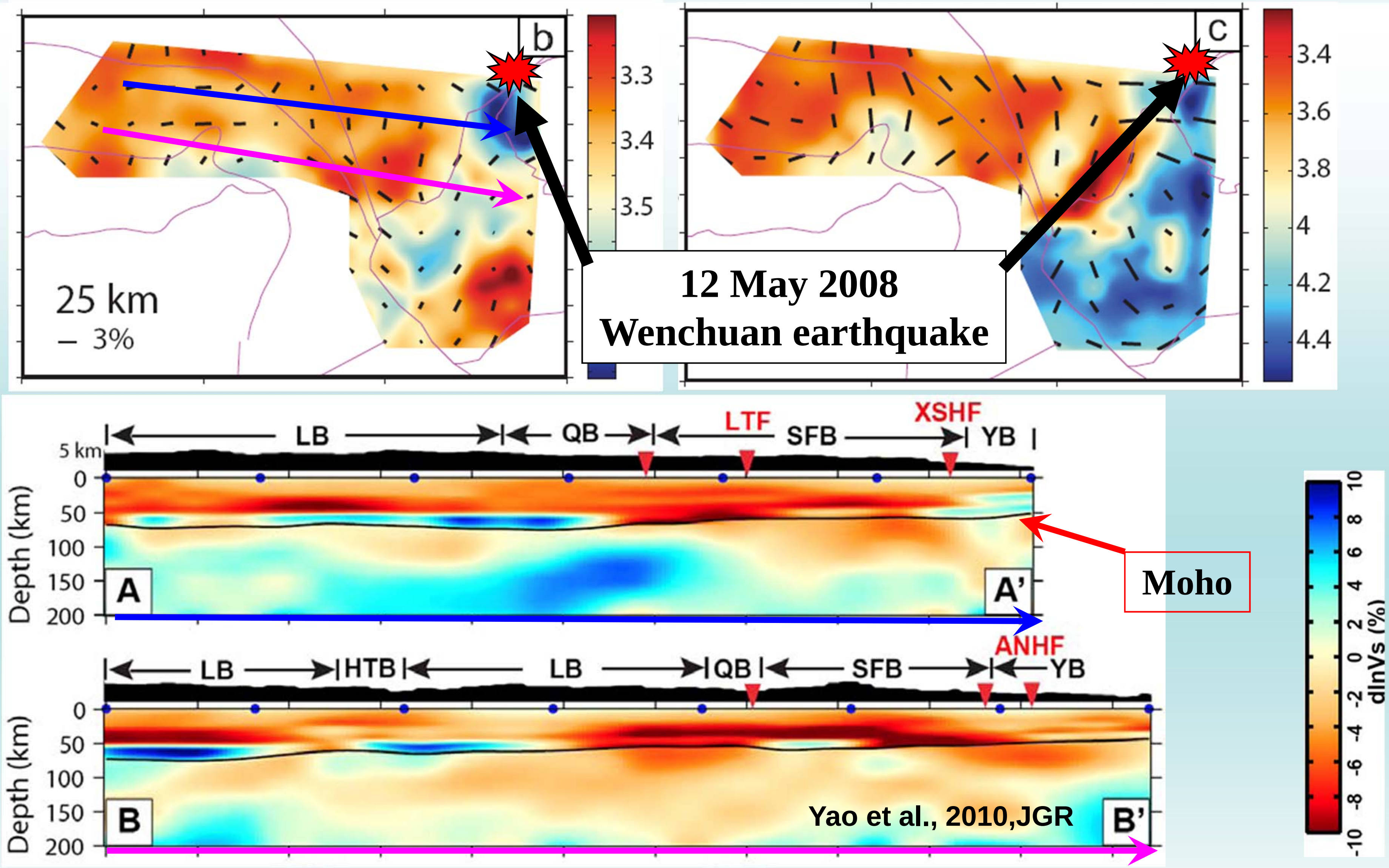

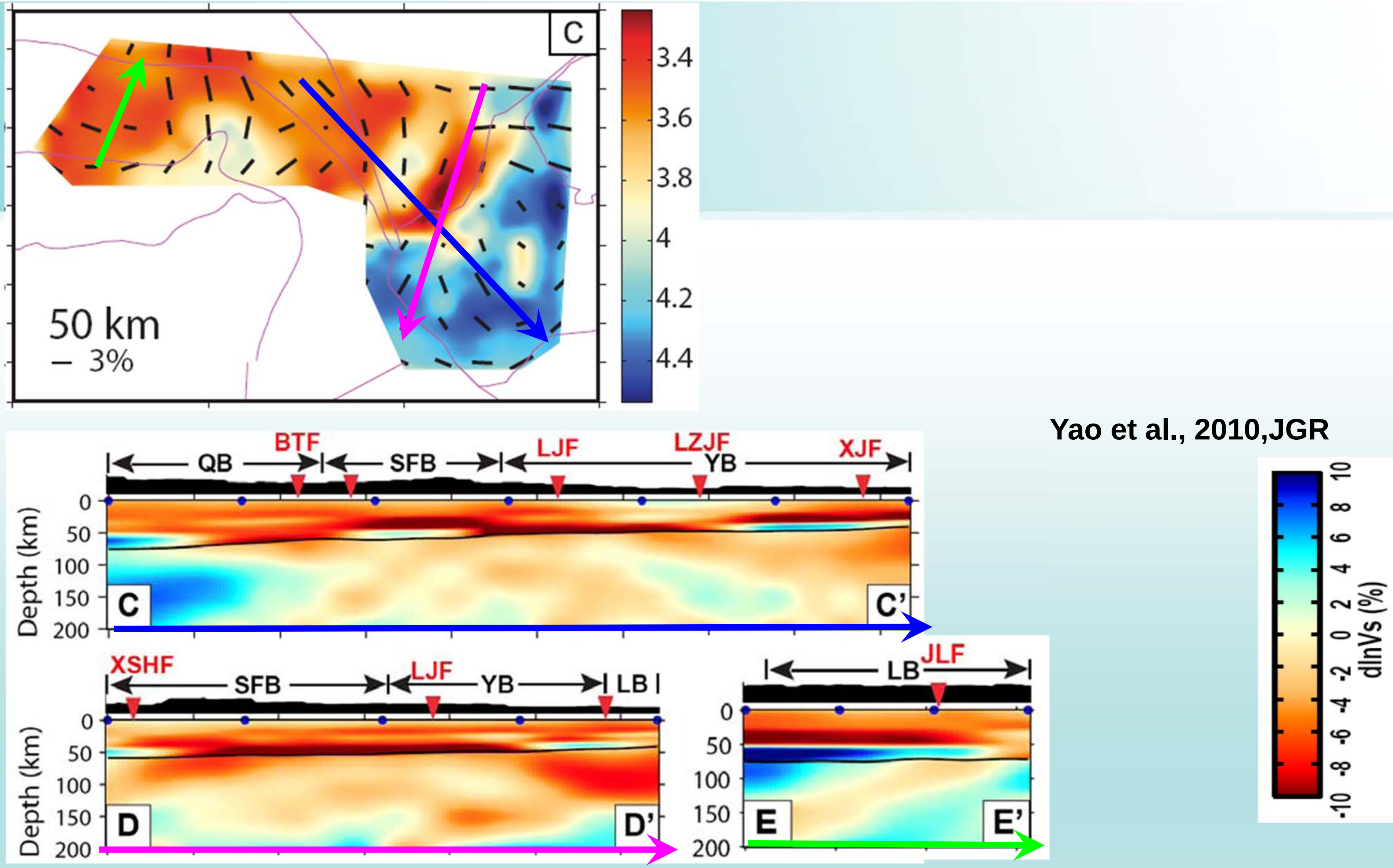

Yao et al., 2010,JGR

- Widespread mid/lower crustal LVZs → possibly mechanically weaker
- Faults may interact with (e.g., truncate) LVZs (need further high resolution studies)
- 3D geometry of LVZs → complicated crustal flow pattern if crustal flow exists

Western Sichuan Dense Array Tomography

Liu Qiyuan et al. (2014, Nature Geoscience)

Joint inversion of ambient noise dispersion (2-40 s) and P wave receiver functions

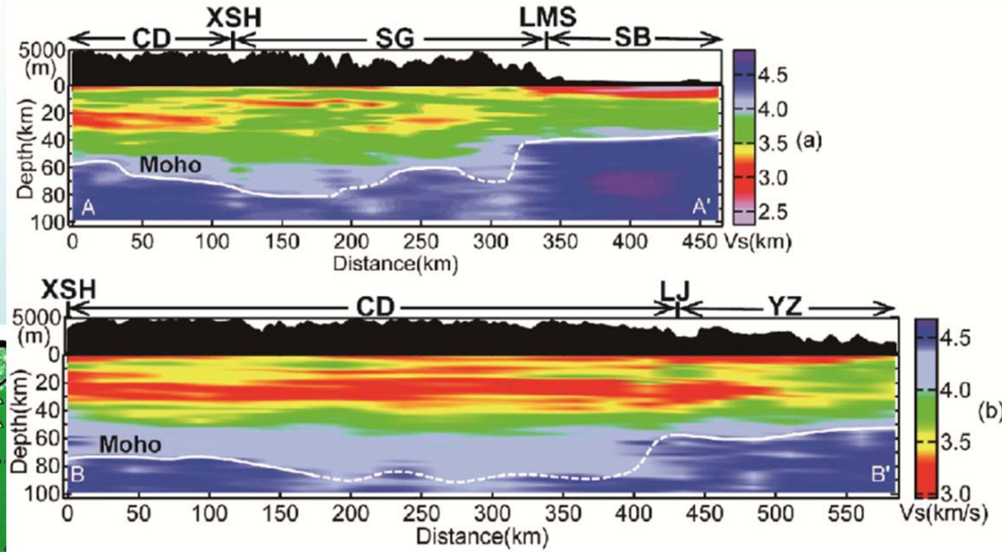

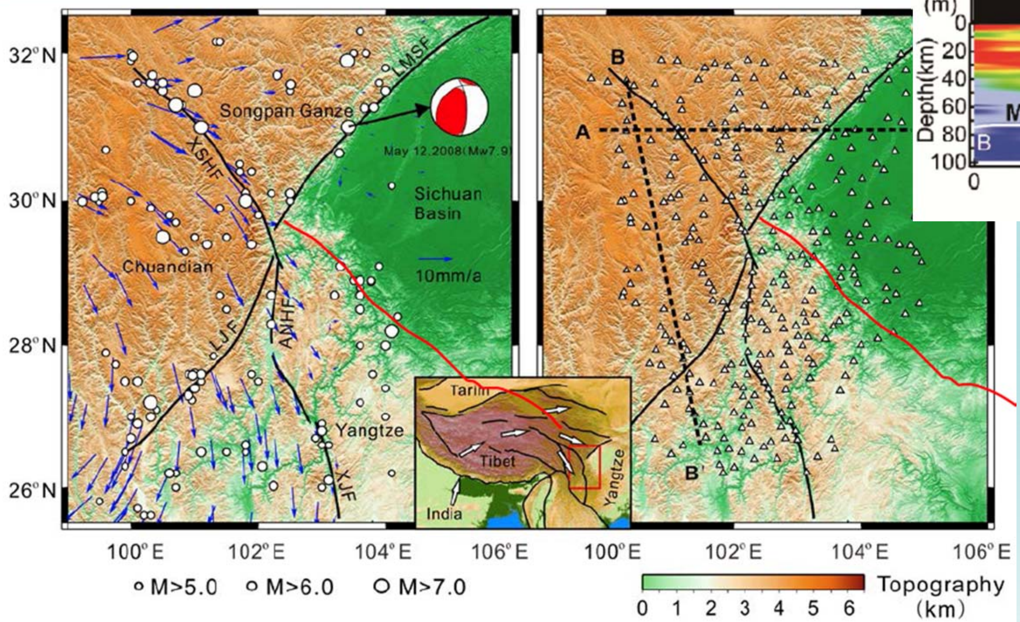

Western Sichuan: mid-crust low velocity layer(LVL), thickened lower crust（Moho is not clear）, interaction between faults and LVL

Eastward expansion of Tibetan plateau is controlled by both crustal flow and strain partitioning across faults

Liu et al. (2014, Nature Geoscience)

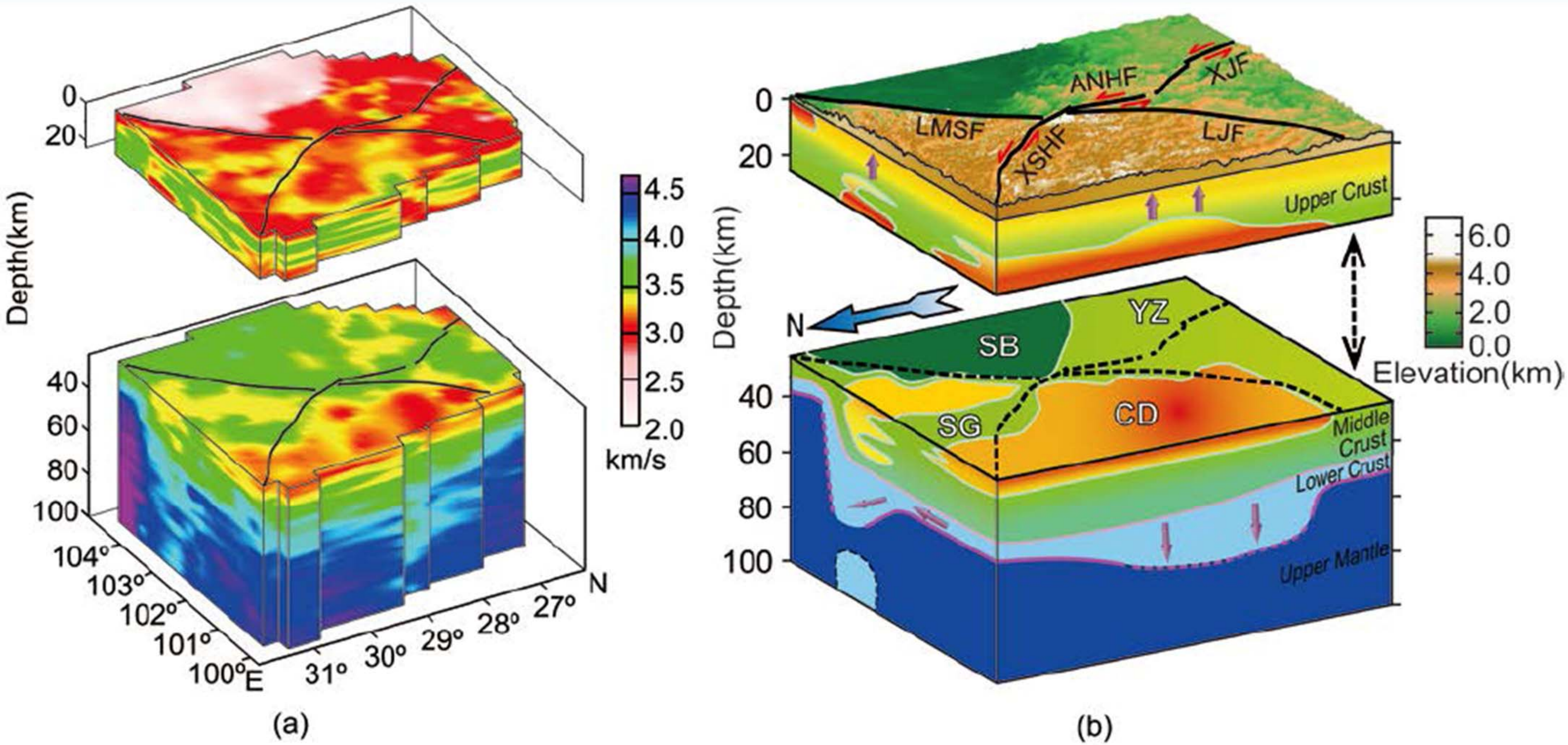

Comparison with other results：

Crustal LVLs revealed by ambient noise tomography in Tibet

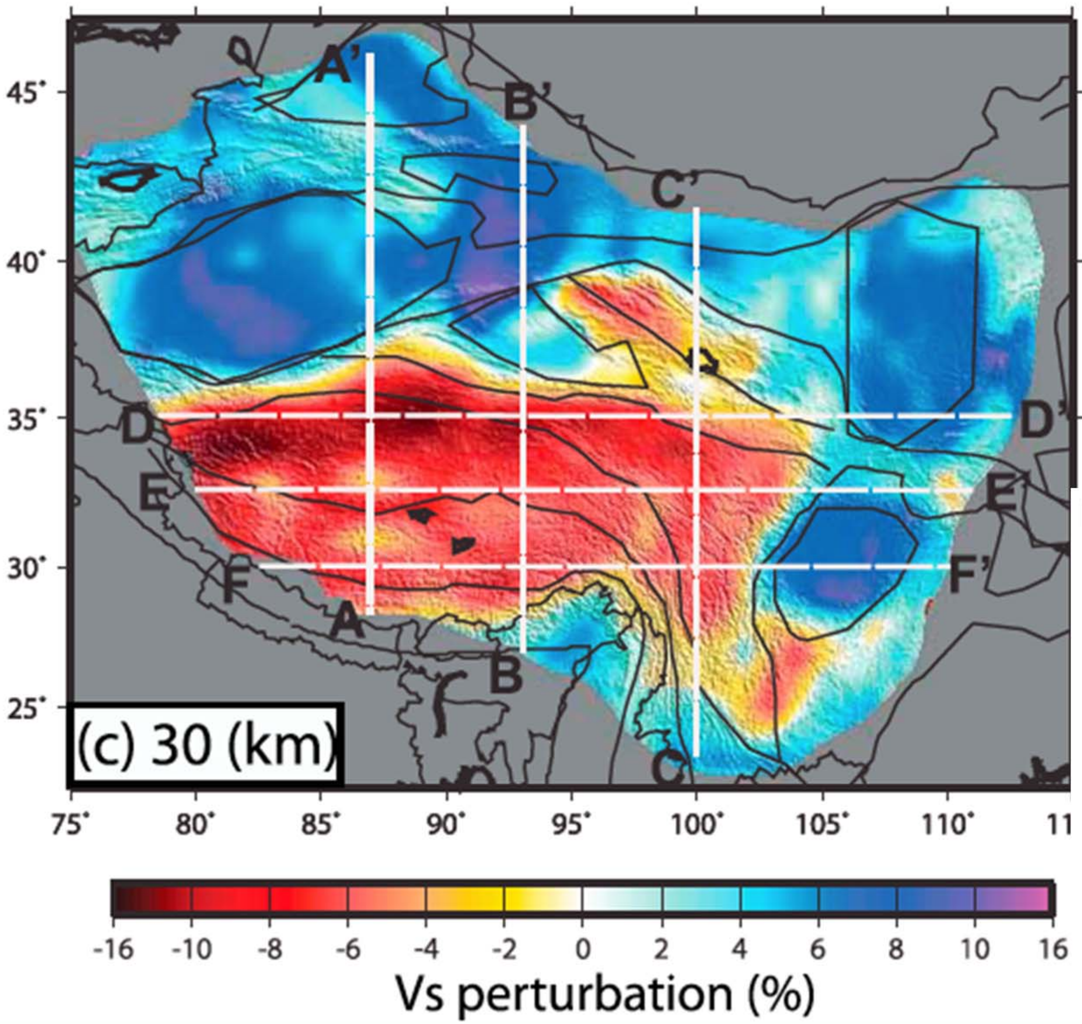

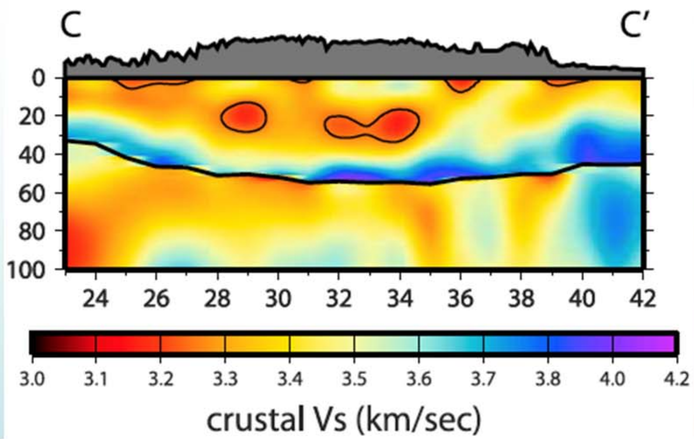

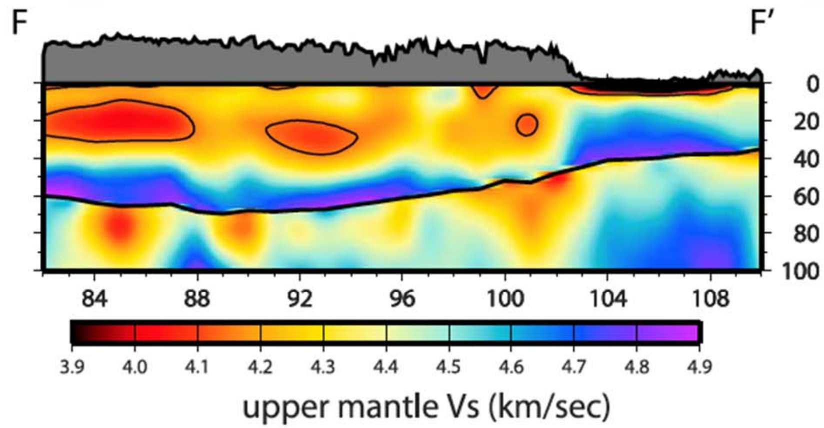

Yang et al. 2012, JGR

Receiver function
Wang et al. EPSL, 2009

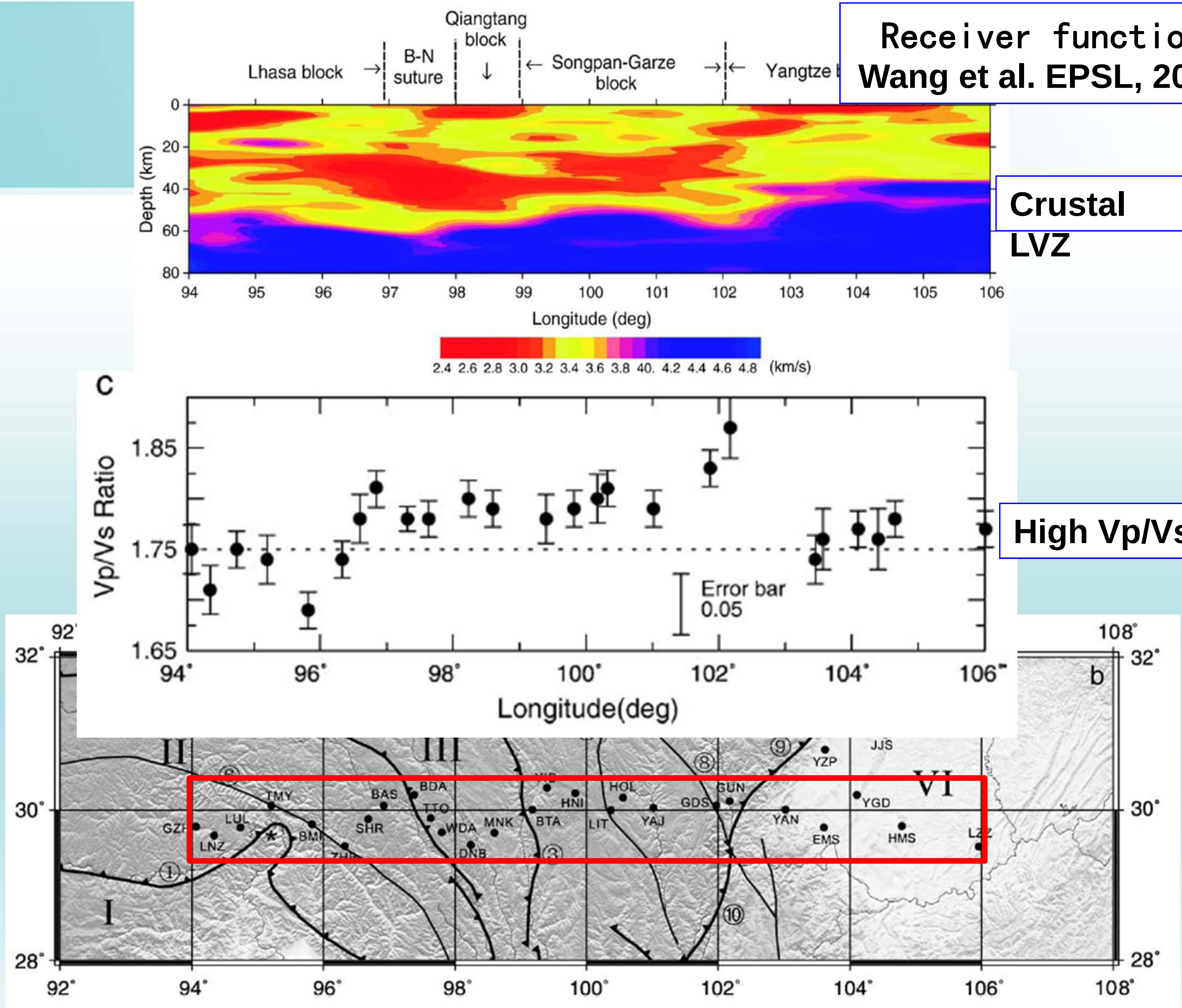

Crustal LVZ

High Vp/Vs

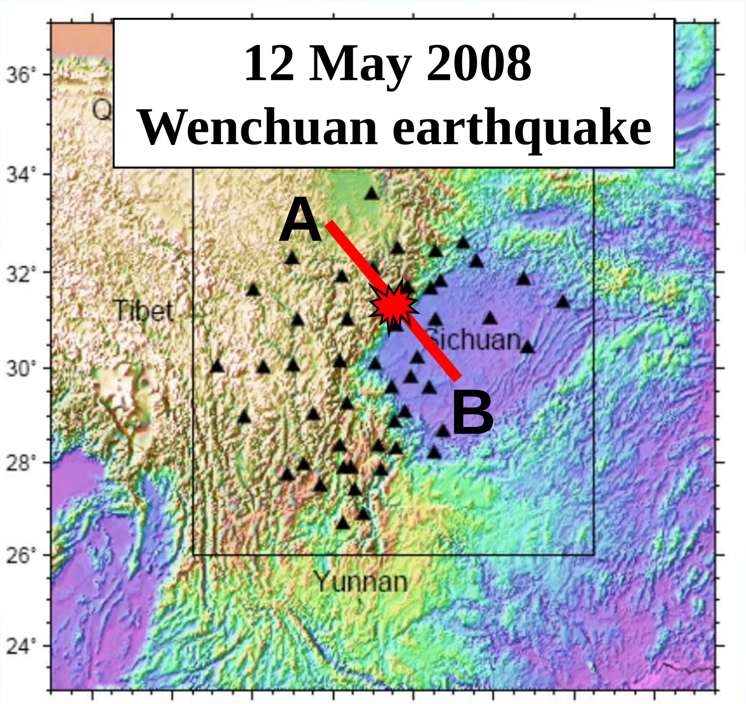

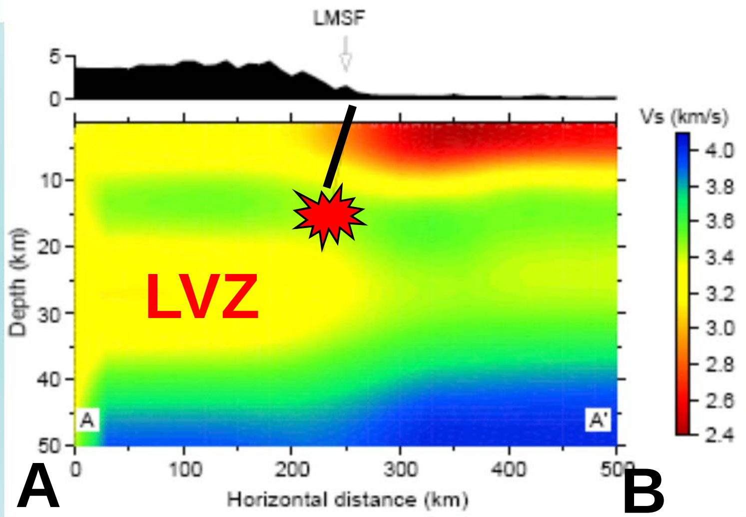

Ambient Noise Analysis
(Li et al, EPSL, 2009)

Receiver Function Analysis
(Liu et al., 2010)

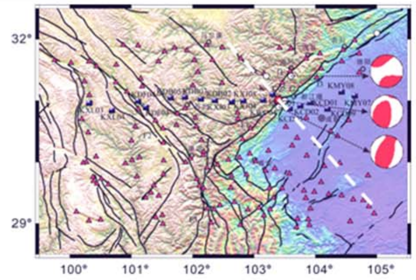

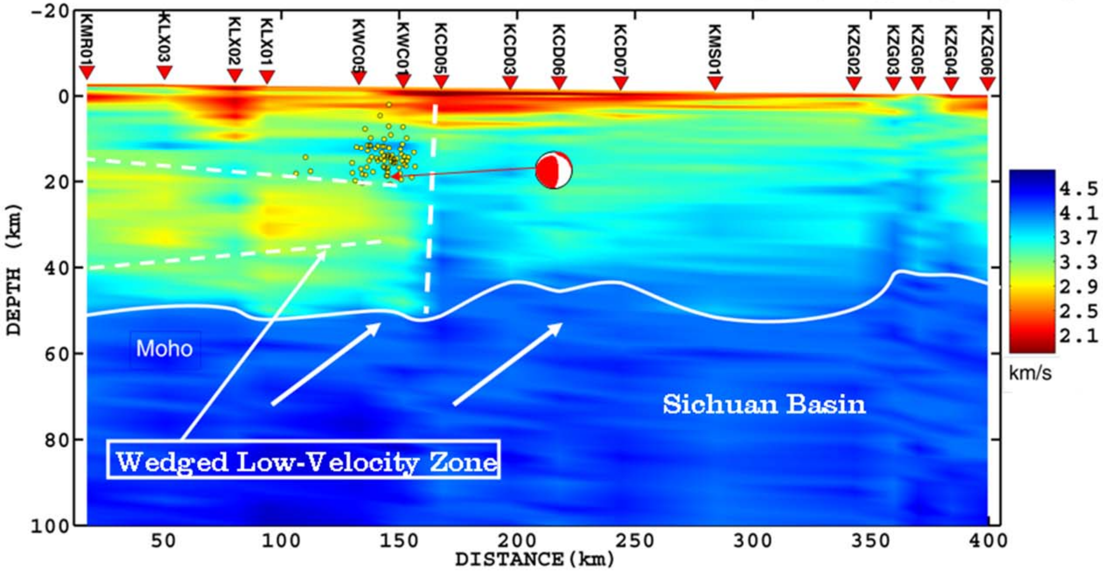

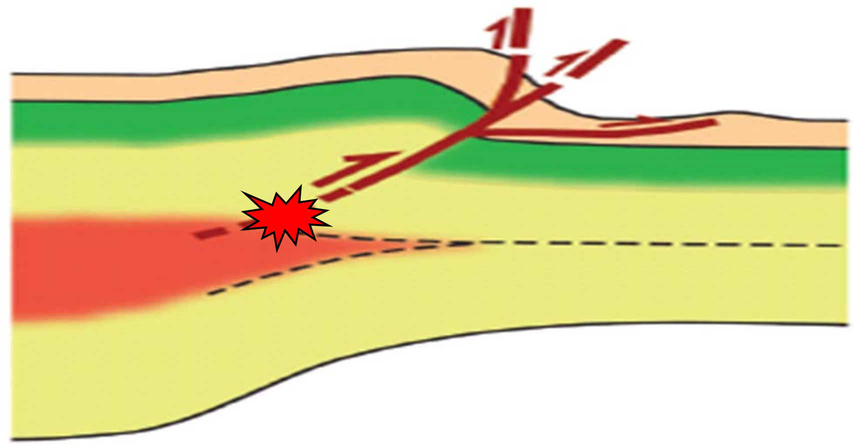

Burchfiel et al. (GSA Today, 2008)

(2) Crustal Radial Anisotropy in SE Tibet and SW China

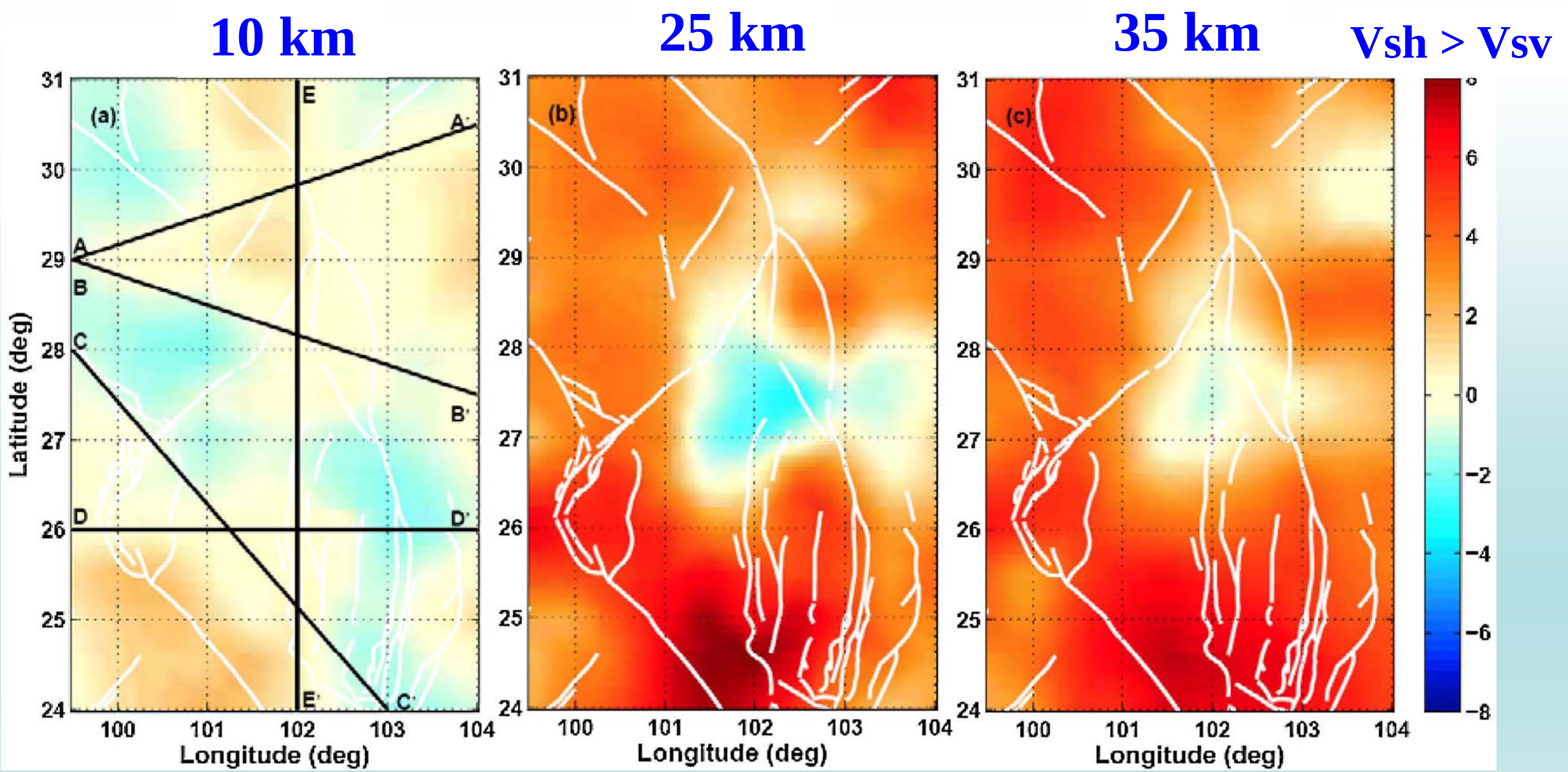

2(Vsh – Vsv)/(Vsh + Vsv)*100%

Huang, Yao, van der Hilst, 2010, GRL

Correlation between LVZ and Radial Anisotropy

Large positive radial anisotropy correlates well with LVZs in the mid/lower crust

Sub-horizontal alignment of anisotropic crustal minerals (e.g., mica, amphibole), consistent with deep crustal flow

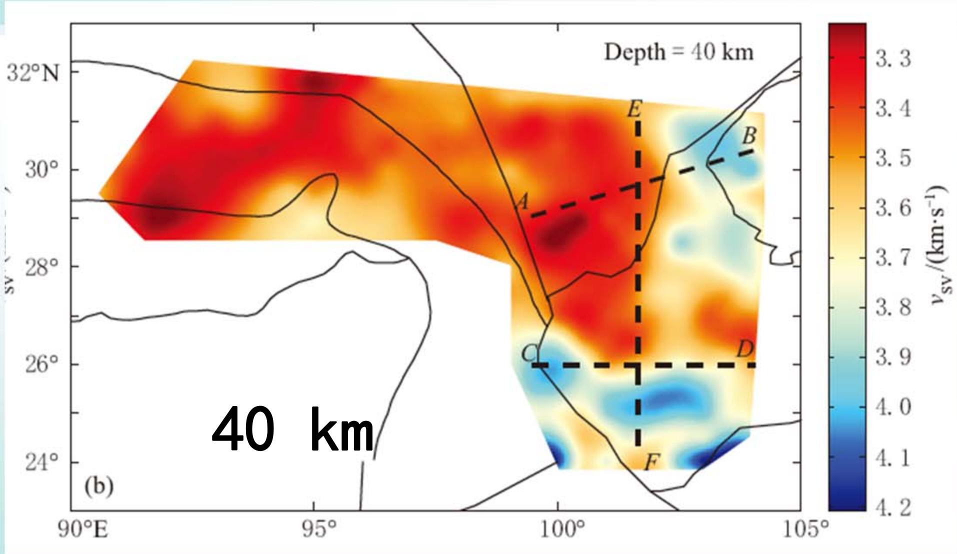

Vsv

2(Vsh – Vsv)/(Vsh+Vsv)

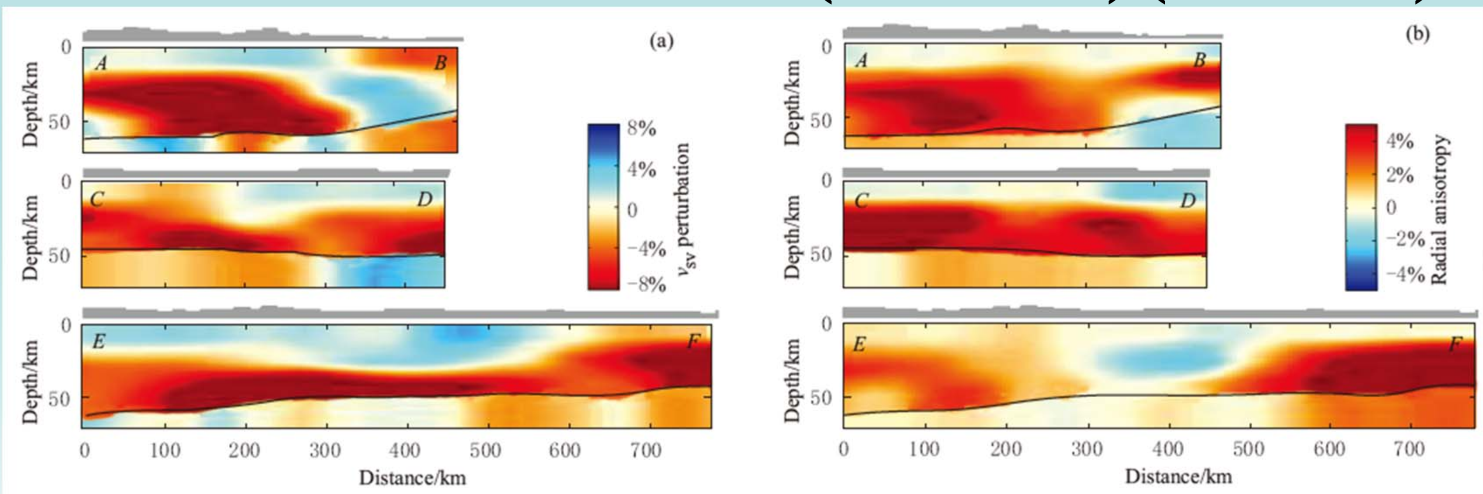

Huang et al. 2010; Yao, 2012

(3) Azimuthal Anisotropy and Lithospheric Deformation

Complicated deformation pattern of crust and upper mantle

Upper crust: consistent with clockwise rotation

Uppermost mantle: fast direction along the LVZ of the margin of Yangtze block

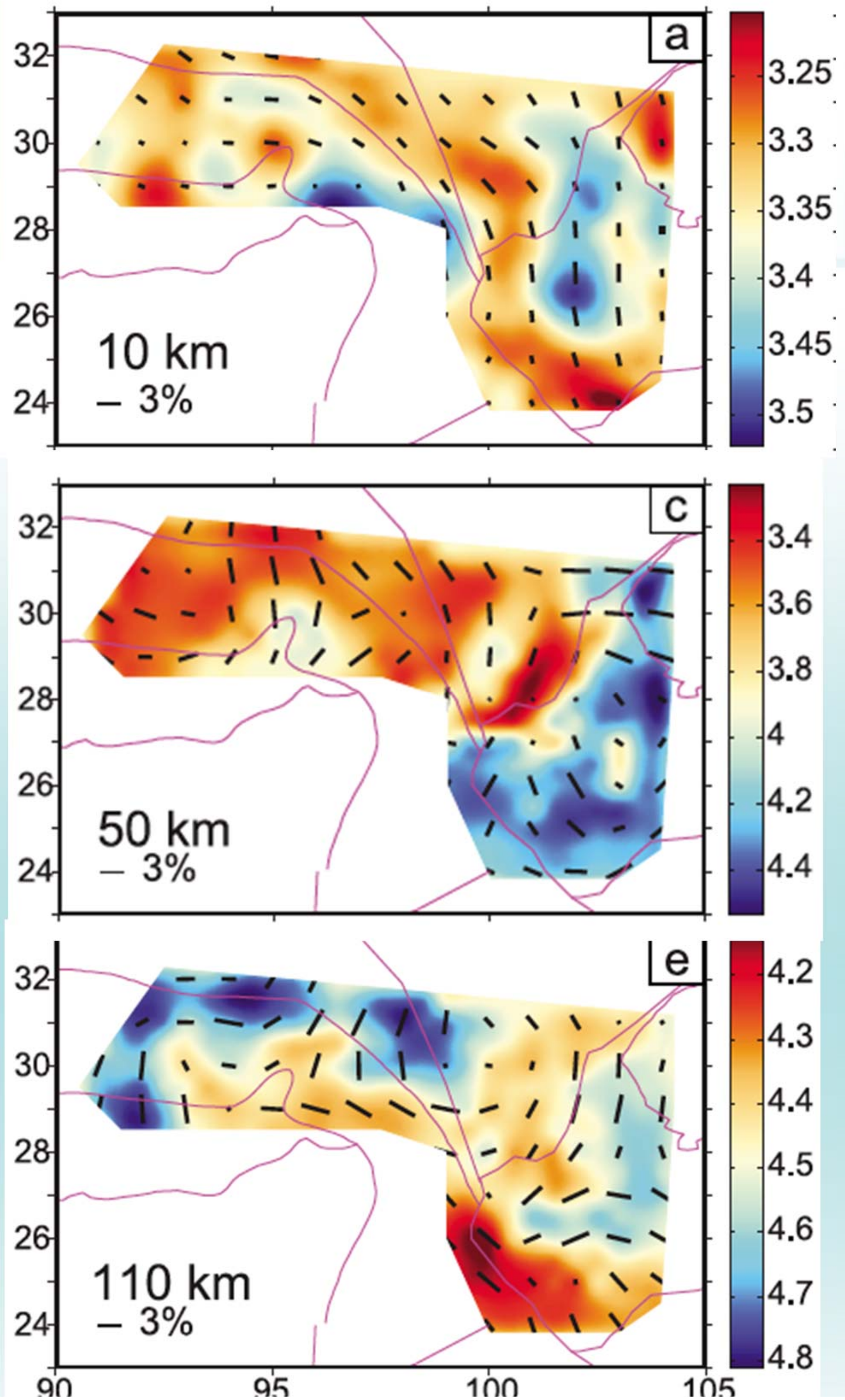

Yao et al., 2010,JGR

Comparison with teleseismic shear wave splitting

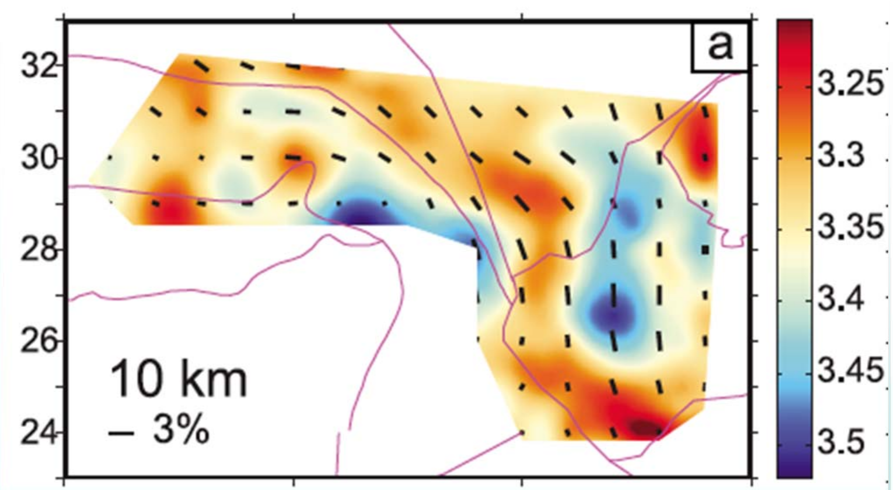

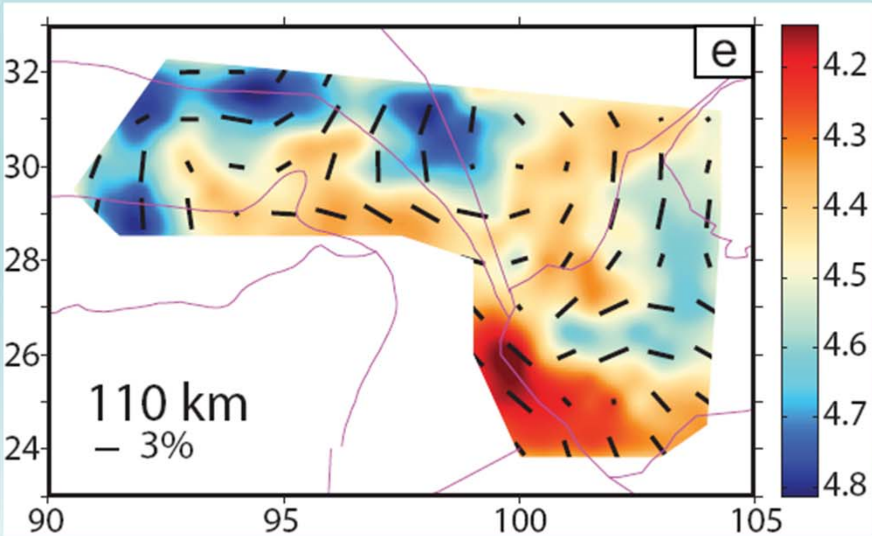

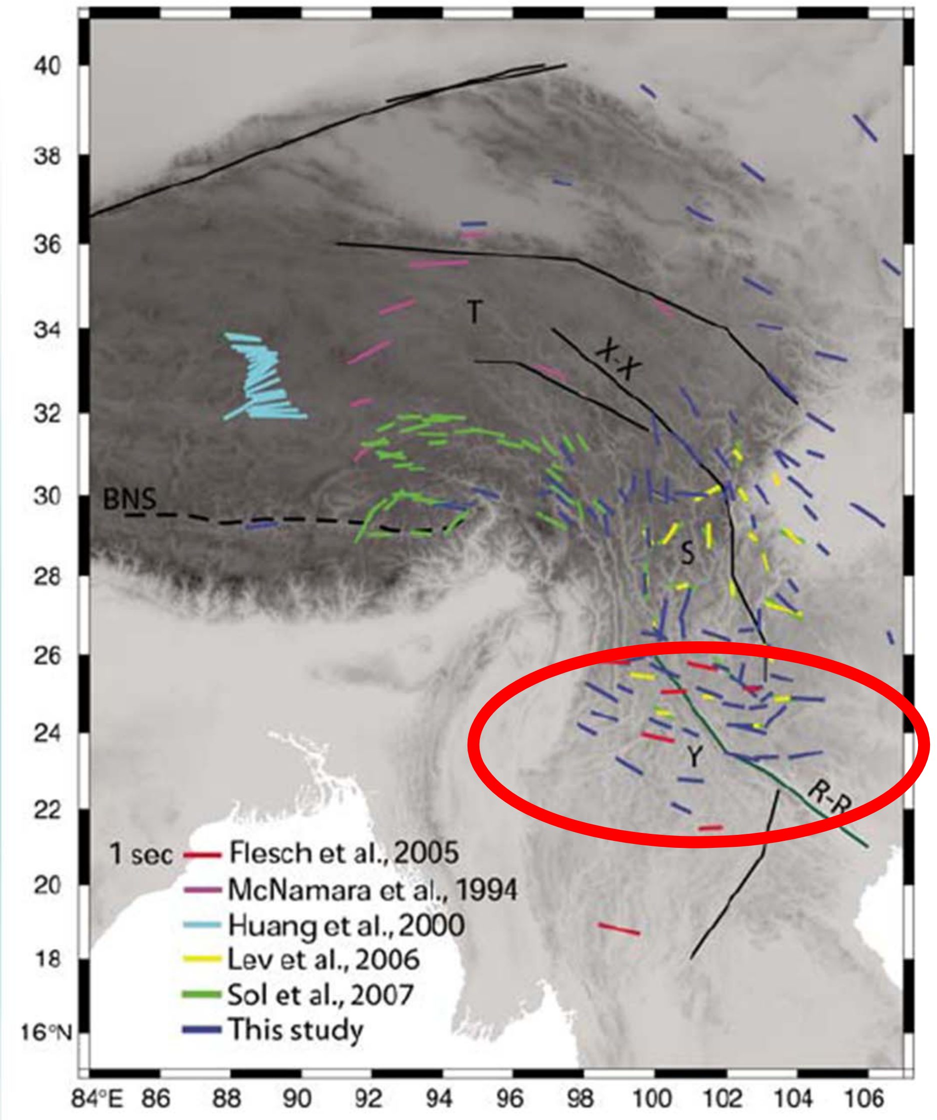

Comparison with body wave tomography

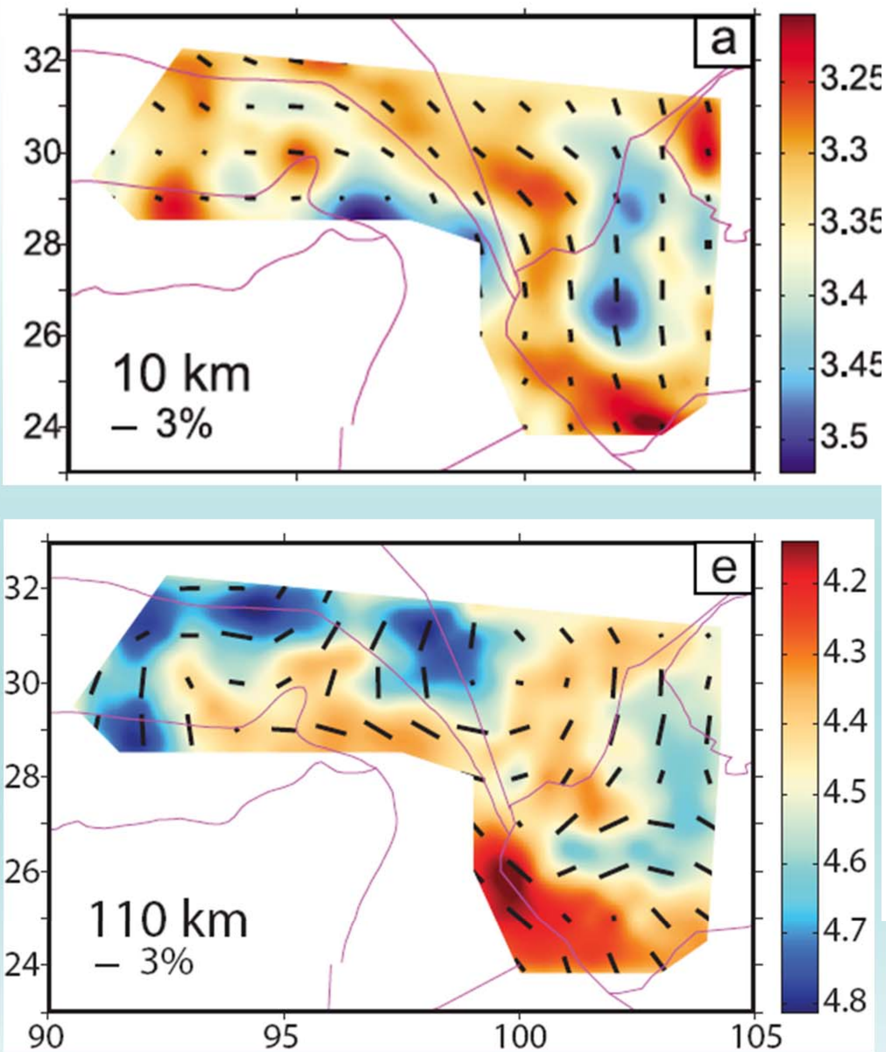

10 km

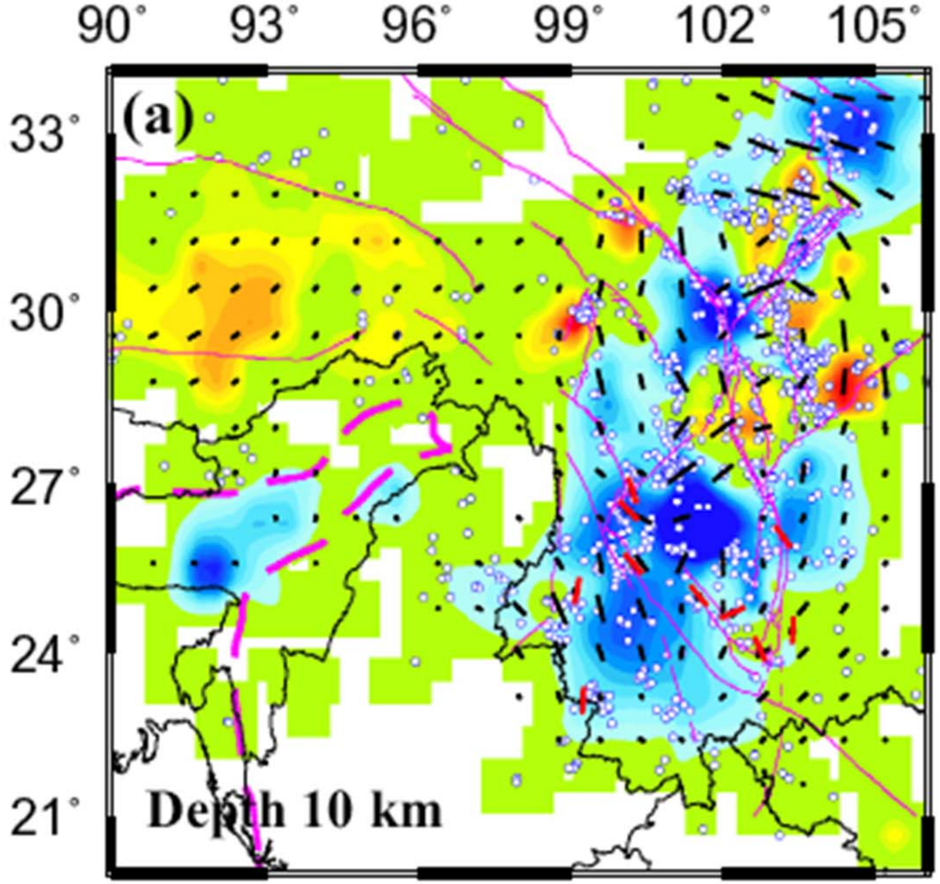

Wei al., 2013, PEPI

Comparison with body wave tomography

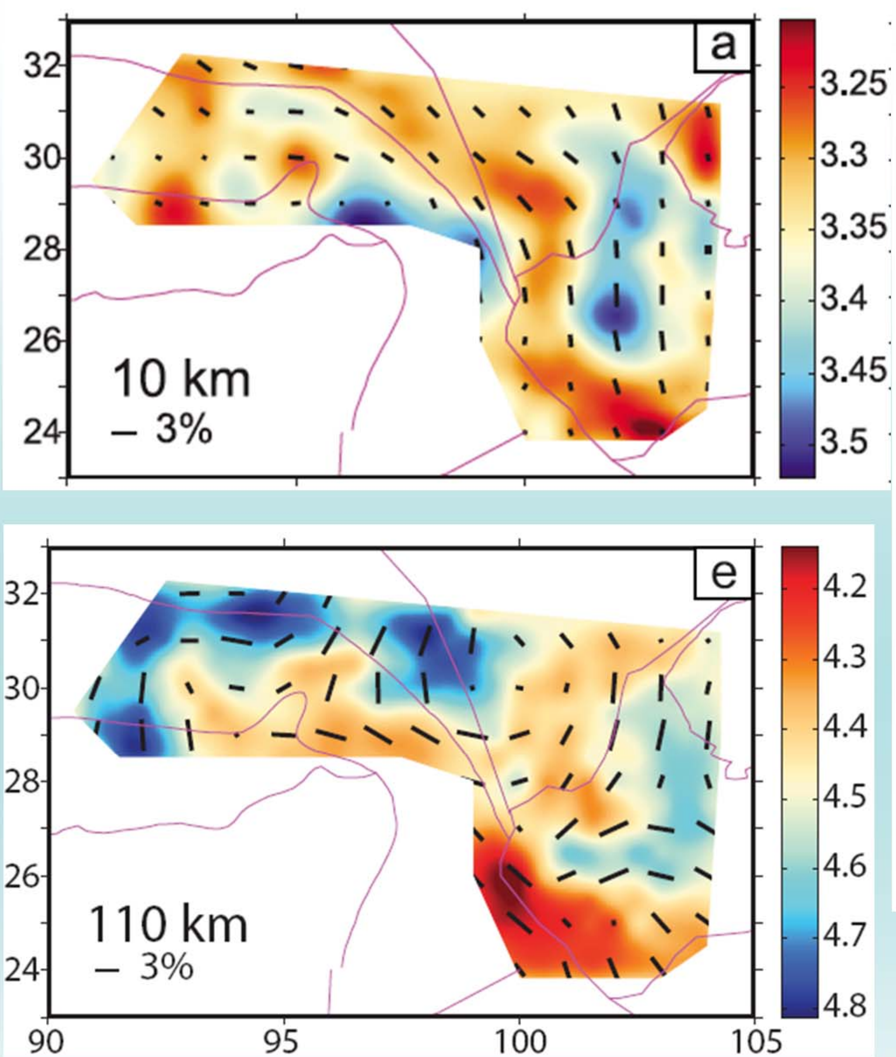

100 km

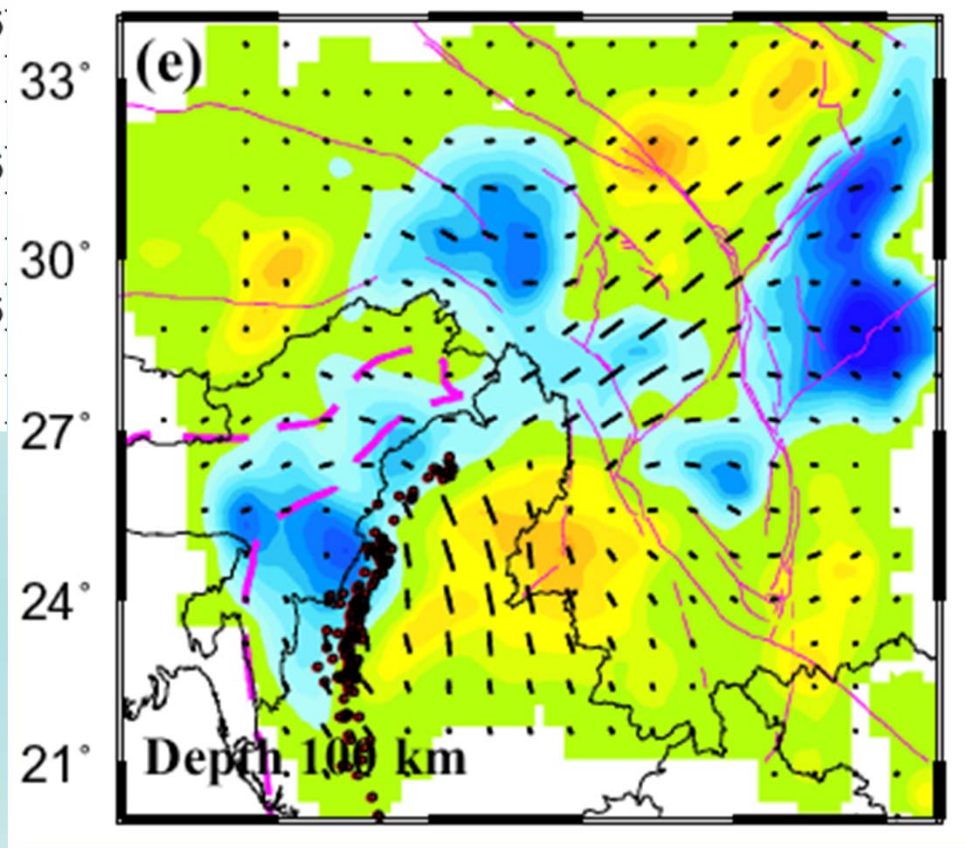

Wei al., 2013, PEPI

Upper crust (10km):fast axes // large strike slip faults
→faults may control upper crust deformation: simple shear

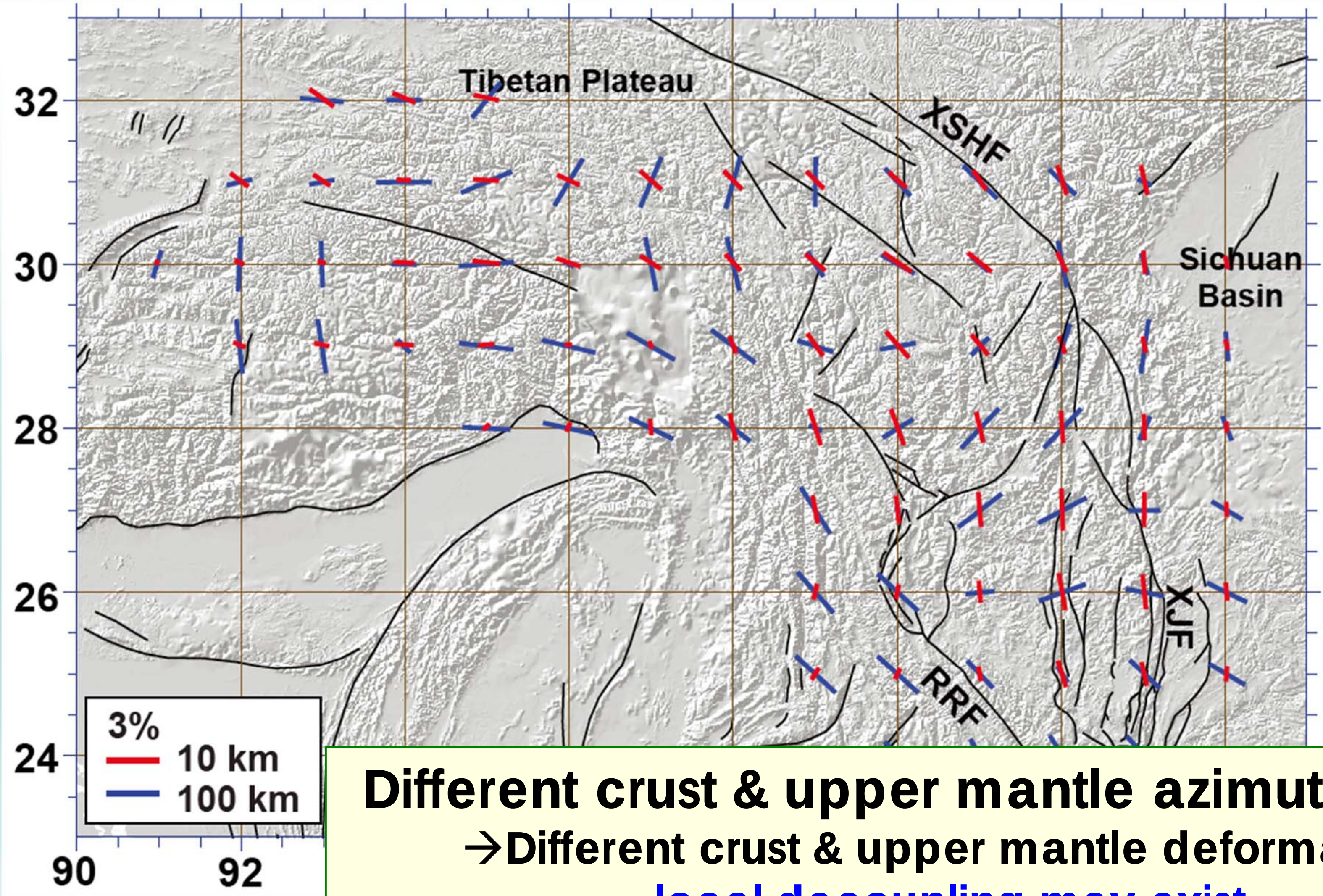

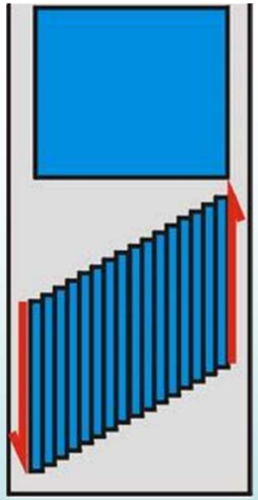

Different crust & upper mantle azimuthal anis.

→Different crust & upper mantle deformation, local decoupling may exist

Yao 2012

(4) Some discussions

Heat flow and Tibetan crust strength

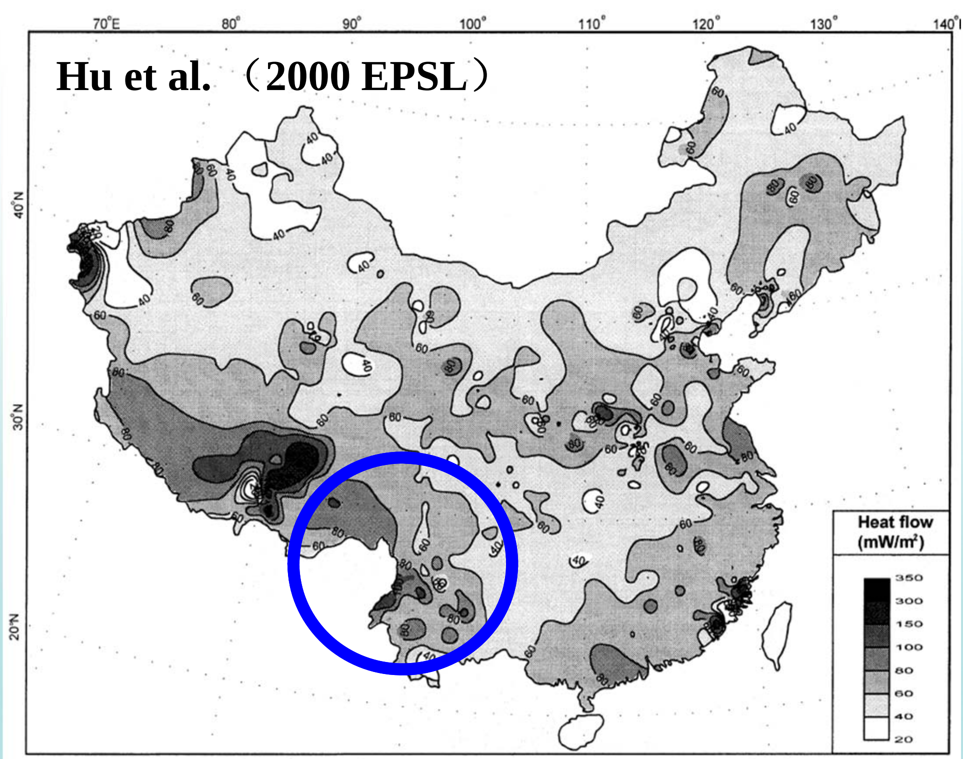

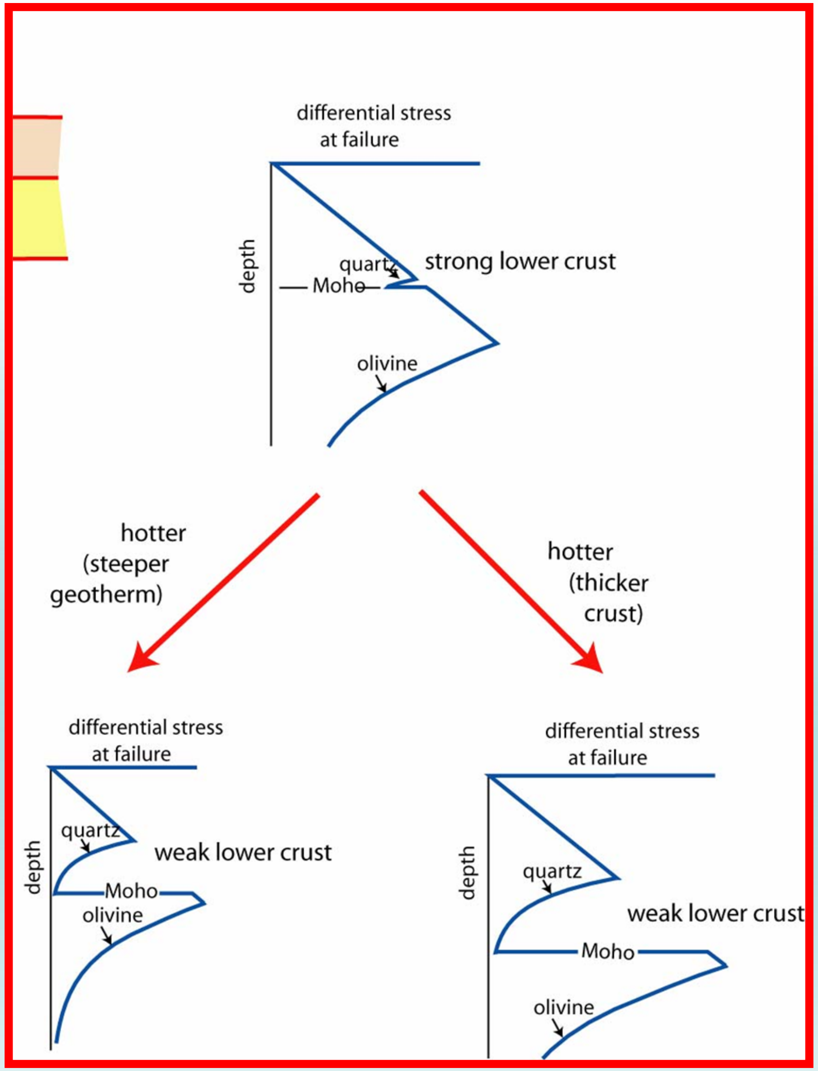

High surface heat flow value

70—80 thick crust

Probably weak mid-lower crust

Tibetan lithosphere effective elastic thickness (Te)

Jordan & Watts （2005, EPSL）

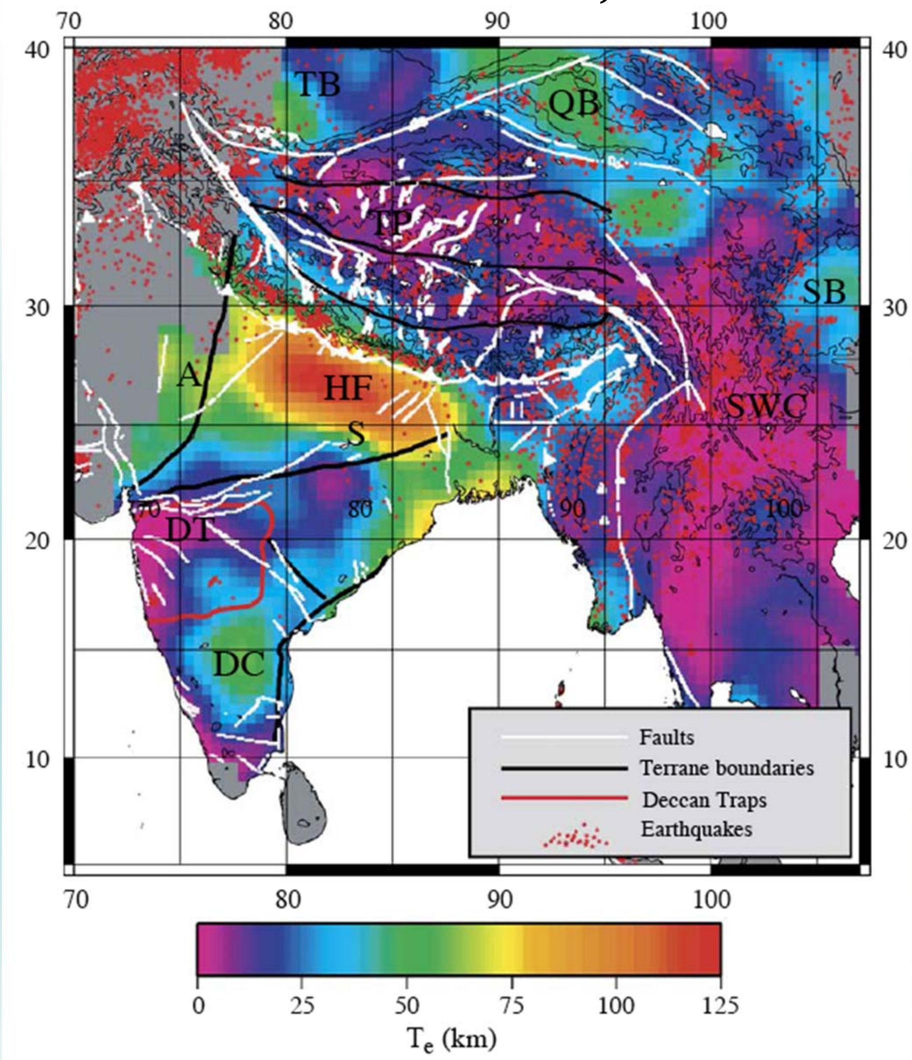

Most regions in Tibet and SW China show very low Te (<10 km):

very weak lithospheric strength

maybe dominated by ductile/plastic deformation

in support of channel flow model

magnetotelluric (MT) imaging: resistivity

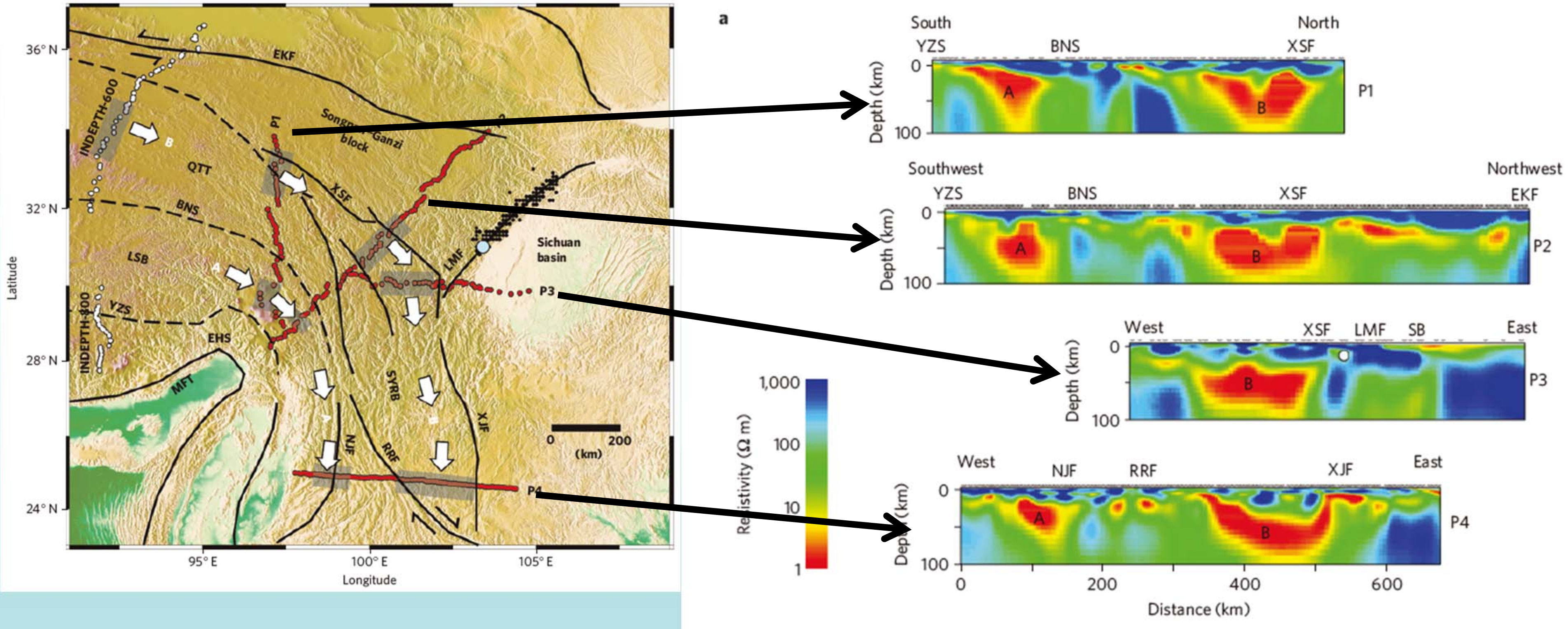

Bai et al. 2010

Two low resistivity channels in the mid-lower crust
Distribution of channels is highly connected to faults

Summary

Southeastern Tibetan Plateau: complicated lithospheric structure and deformation patterns

Simple end member model (e.g., rigid block extrusion or lower crust channel flow) is difficult to explain all the geophysical observations!

We need a more sophisticated model for SE Tibet lithospheric deformation!

Summary: southeastern Tibetan Plateau structure and deformation

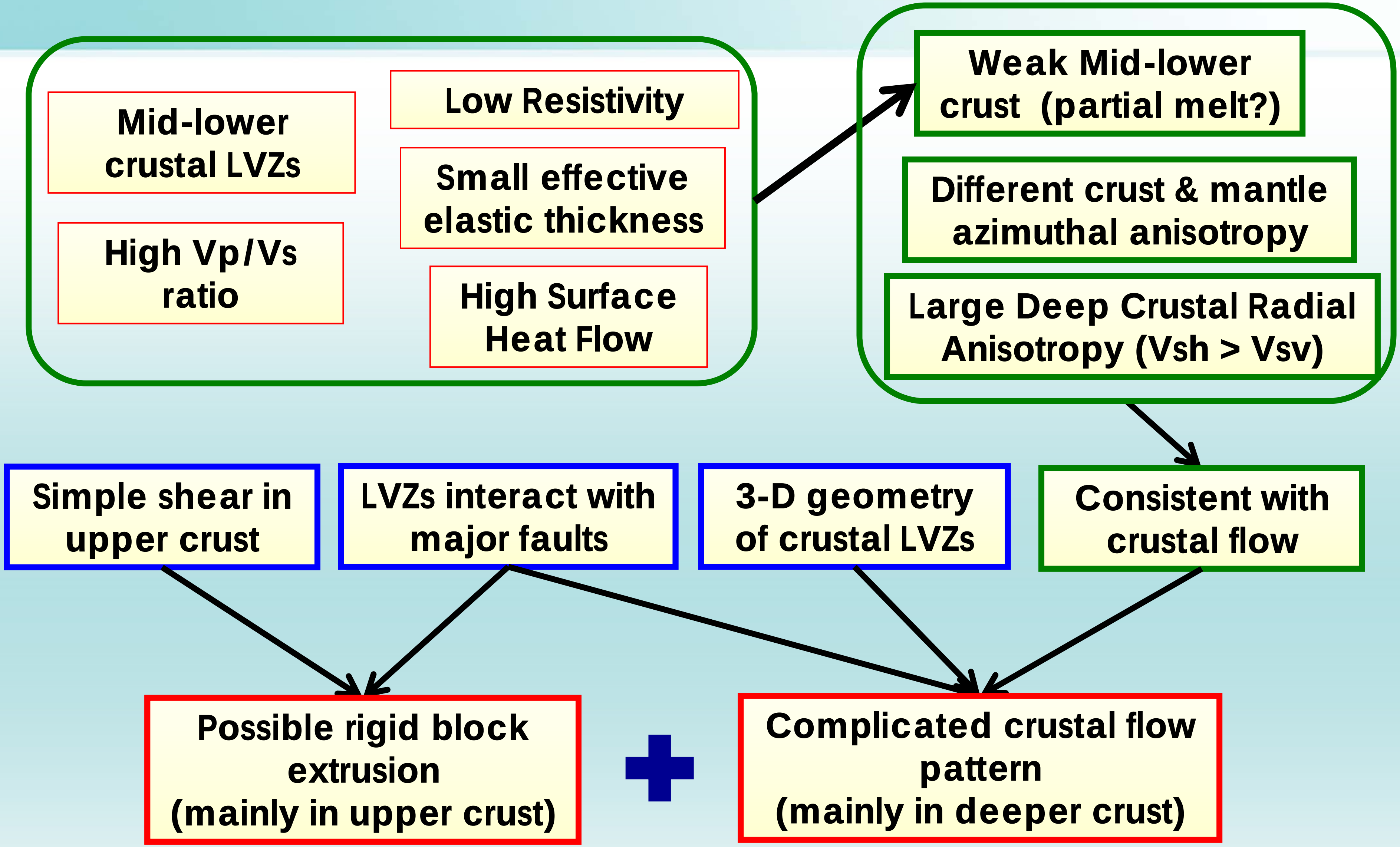


Thank you!
Welcome to Hefei

Effects of uneven noise distribution on tomography

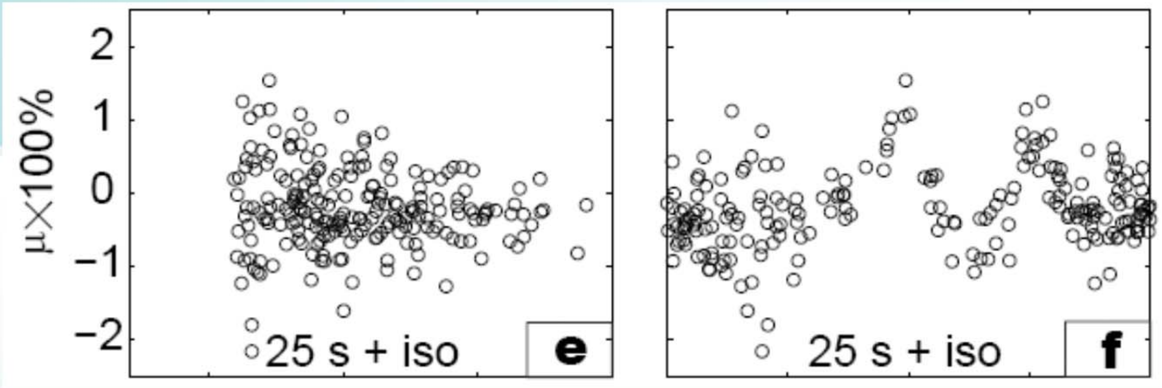

$$C(\theta,\varphi,\psi) = C_0(\theta,\varphi)\{1 + A(\theta,\varphi)\cos(2\psi) + B(\theta,\varphi)\sin(2\psi)\}$$